Physical Control of the Distributions of a Key Arctic Copepod in the Northeast Chukchi Sea

by

Stephen M. Elliott

B.S., United States Coast Guard Academy (2005)

Submitted in partial fulfillment of the requirements for the degree of
Master of Science in Mechanical Engineering
at the
MASSACHUSETTS INSTITUTE OF TECHNOLOGY
and the
WOODS HOLE OCEANOGRAPHIC INSTITUTION
June 2015

Author: Signature redacted
Department of Mechanical Engineering
Department of Applied Ocean Science and Engineering
May 14, 2015

Certified by: Signature redacted
Dr. Carin J. Ashjian
Senior Scientist
Thesis Supervisor
Woods Hole Oceanographic Institution

Certified by: Signature redacted
Dr. Pierre F.J. Lermusiaux
Associate Professor of Mechanical Engineering
Thesis Reader

Accepted by: Signature redacted
Dr. Henrik Schmidt
Professor of Mechanical and Ocean Engineering
Chair, Joint Committee for Applied Ocean Science and Engineering

Accepted by: Signature redacted
Dr. David E. Hardt
Professor of Mechanical Engineering
Chair, Mechanical Engineering Committee on Graduate Students

Physical Control of the Distributions of a Key Arctic Copepod in the Northeast Chukchi Sea

by

Stephen Malcolm Elliott

Submitted to the Department of Mechanical Engineering and
Department of Applied Ocean Science and Engineering
on May 14, 2015, in partial fulfillment of the
requirements for the degree of
Master of Science

Abstract

The copepod *Calanus glacialis* is one of the most important zooplankton taxa in the Arctic shelf seas where it serves as a key grazer, predator, and food source. Its summer distribution and abundance has direct effects on much of the food web, from blooming phytoplankton to migrating bowhead whales. The Chukchi Sea represents a highly advective regime dominated by a barotropicly driven northward flow modulated by wind driven currents that reach the bottom boundary layer of this shallow environment. In addition, a general northward gradient of decreasing temperature and food concentration leads to geographically divergent copepod growth and development rates. The physics of this system establish the connection potential between specific regions. Unless biological factors are uniform and ideal the true connections will be an uneven subset of this physically derived connection potential. In August 2012 and 2013, *C. glacialis* distributions were observed over Hanna Shoal in the northeast Chukchi Sea. Here we used the Finite Volume Community Ocean Model i-State Configuration Model to advect these distributions forward and back in time to determine the source and sink regions of the transient Hanna Shoal *C. glacialis* population. We found that Hanna Shoal supplies diapause competent *C. glacialis* to both the Beaufort Slope and the Chukchi Cap, mainly receives juveniles from the broad slope between Hanna Shoal and Herald Canyon and receives second year adults from as far as the Anadyr Gulf and as close as the broad slope between Hanna Shoal and Herald Canyon. These connection potentials were not sensitive to precise times and locations of release, but were quite sensitive to depth of release. Deeper particles often traveled further than shallow particles due to strong vertical shear in the shallow Chukchi. The 2013 sink region was shifted west relative to the 2012 region and the 2013 adult source region was shifted north relative to the 2012 region.

Thesis Supervisor: Dr. Carin J. Ashjian
Title: Senior Scientist
Woods Hole Oceanographic Institution

Acknowledgements

As this project finally bears fruit I have the chance to recognize that none of this would have been possible without the amazing support of myriad people and organizations.

I would like to thank The United States Coast Guard for the time and much of the funding needed to further my education in a field for which I have a great deal of passion. Thanks to Dr. John Berkson for his coordination, support and flexibility. I would never have entered the WHOI Joint Program were it not for my advisor, Dr. Carin Ashjian, who told me as chief scientist on USCGC HEALY in 2007 that I should contact her if I ever needed anything. Thanks also to Jim Preisig and Andone Lavery for their encouragement as well as the Academics Programs Office for the generous offer that allowed me to attend the most prestigious marine science institution in the country.

The U.S. Department of Interior, Bureau of Ocean Energy and Management (BOEM), Alaska Outer Continental Shelf Region, Anchorage, Alaska provided funding for the fieldwork and plankton sample enumeration as part of the Chukchi Sea Offshore Monitoring in Drilling Area (COMIDA) Project and the BOEM Alaska Environmental Studies Program under contract Number M11AC00007 to the University of Texas and a subcontract to the Woods Hole Oceanographic Institution.

The execution of this project was not individual effort. First and foremost Carin's guidance, advice and encouragement kept me grounded and on track. The crew of USCGC HEALY was instrumental in completing the fieldwork. Phil Alatalo taught me the dark arts of Arctic zooplankton sampling and kept me in line on the night watch. Dr. Changsheng Chen from UMASS Dartmouth generously offered the AO-FVCOM output that I used to drive FISCM. Jason Boucher and Yu Zhang helped me get the output and understand it. Dr. Zhixuan Feng was an excellent sounding board and was invaluable in helping me understand FISCM's FORTRAN code. Dr. Rubao Ji, Xuezhu Lyu and Dr. Yun Li all gave me great advice as the work developed. Particular credit must be given to Benjamin Jones for always having time for my silly modeling questions. Dr. Thomas Weingartner and Ying-Chih Fang from the University of Alaska Fairbanks provided data, codes and advice as to the physical oceanography of the Chukchi. From MIT, Dr. Pierre Lermusiaux's instruction on computational fluid mechanics as well as his positivity and recommendations were key.

The thesis itself was only part of my graduate school experience. Many thanks to Sydney Sroka, Margaux Filippi, Jennifer Landry, Pedro Vaz Teixeira and Zhibiao Rao for pseting with me, often until the wee hours of the morning. Without their help, explanations and encouragement there is no way I could have completed my required coursework.

I would like to thank my parents Glenn and Nancy Elliott for their encouragement, support and love that have followed me through my entire life, no matter the pursuit. My wife Jennifer Ah-King Elliott has been an inspiration. It has only been through her support, both direct and indirect, that I have reached the end of this particular path.

Finally I dedicate this thesis to my grandfather Dr. James R. Moulton, a marine scientist whom I was never able to get to know, but whose passion for the sea did his daughter lovingly pass on to me.

Contents

List of Figures

List of Tables

Chapter 1

Introduction

Hanna Shoal in the northeastern Chukchi Sea is a highly productive region that, like much of that shallow arctic shelf sea, exhibits abnormally tight pelagic-benthic coupling and supports a rich population of pinnipeds (Hunt et al., 2013). The scale of this coupling is emphasized by Mathis and Questel (2013). They found that an area roughly half the size of Hanna Shoal exported over 340,000 kg of carbon from the atmosphere to the benthos over the course of the 2010 summer. The shoal's shallow depths and promising geology have led it to be a principal target of oil and gas corporations looking to exploit reserves that are now seen as more accessible due to the reduced duration of seasonal ice coverage and advances in offshore drilling technology. In an effort to balance economic interests with a desire to minimize impacts on the environment, The Bureau of Ocean Energy Management (BOEM) has commissioned significant research efforts to better understand the ecosystem over and around Hanna Shoal (BOEM, 2015).

Calanus glacialis is one of the most important grazers in the Arctic zooplankton community in terms of biomass, and its role as an energy concentrator is essential for ecosystem function (Falk-Petersen et al., 2009). This relatively long-lived planktonic crustacean is present over Hanna Shoal in August in all of its life stages and may serve as an important food source for migrating bowhead whales in the fall (Quakenbush et al., 2010). The eastern Chukchi Sea is a dynamic region in terms of its physical oceanography. It is generally characterized by a mean northward flow from Bering Strait, but its shallow nature leads wind driven modulations of this pattern to be very important. Given this highly advective regime, *C. glacialis* populations in the western Arctic are impacted by the success of populations in the Chukchi, while populations in the Chukchi are dependent on the success of populations in the Anadyr Gulf and the rest of the Northern Bering Sea. We need to better understand the physical processes that mediate these connections. To predict the strength of the *C. glacialis* population over Hanna Shoal and to predict the effects of this population on those in the western Arctic, we must know the following: Where are the strongest upstream sources of the *C. glacialis* population over Hanna Shoal and where are the strongest downstream sinks?

The remote and harsh nature of the northeast Chukchi Sea makes long-term spatially widespread data difficult and expensive to obtain, thus using direct observation to find source and sink regions is currently impractical. Coupling field observations with oceanographic models is a way to extrapolate on the limited data that can be collected in order to make broader conclusions. Cruises on USCGC HEALY in August of 2012 and 2013 collected extensive observations of *C. glacialis* across Hanna Shoal along with even higher resolution hydrographic measurements. Simultaneously, Chen et al. were working on a high-resolution version of their Arctic Ocean Finite Volume Community Ocean Model (AO-FVCOM). This model was validated during the winter of 2014 and forcing data is currently available through December 2013. This presented

an excellent opportunity to use a new model combined with field observations to address our question regarding sources and sinks of Hanna Shoal *C. glacialis* populations.

Here we used an individual based model (the FVCOM i-State Configuration Model (FISCM) from Cowles et al.) to advect the observed *C. glacialis* communities forward and backward in time to determine the geographic regions with tight links to Hanna Shoal. We inspected the interannual stability of these linkages, as well as their sensitivity to sampling location, time and depth. This allows us to draw insight as to whether interannual differences in the observed populations are due more to differences in advective pathways or differences in biological and physical conditions in source regions. It also allows us to identify the persistent physical oceanographic features critical to controlling the distribution of *C. glacialis* in the northeast Chukchi Sea.

Chapter 2

Background and Literature Review

2.1 Physical Environment

The Chukchi Sea is a dynamic, shallow, marginal sea where water masses from the Pacific, Atlantic and Arctic Oceans meet, resulting in a complex and highly productive ecosystem. The mean circulation pattern of the Chukchi Sea is generally northward (Figure 2-1). Hanna Shoal, the focus of this project, can be seen in the northeast corner of the sea on the edge of the Canada Basin of the Arctic Ocean.

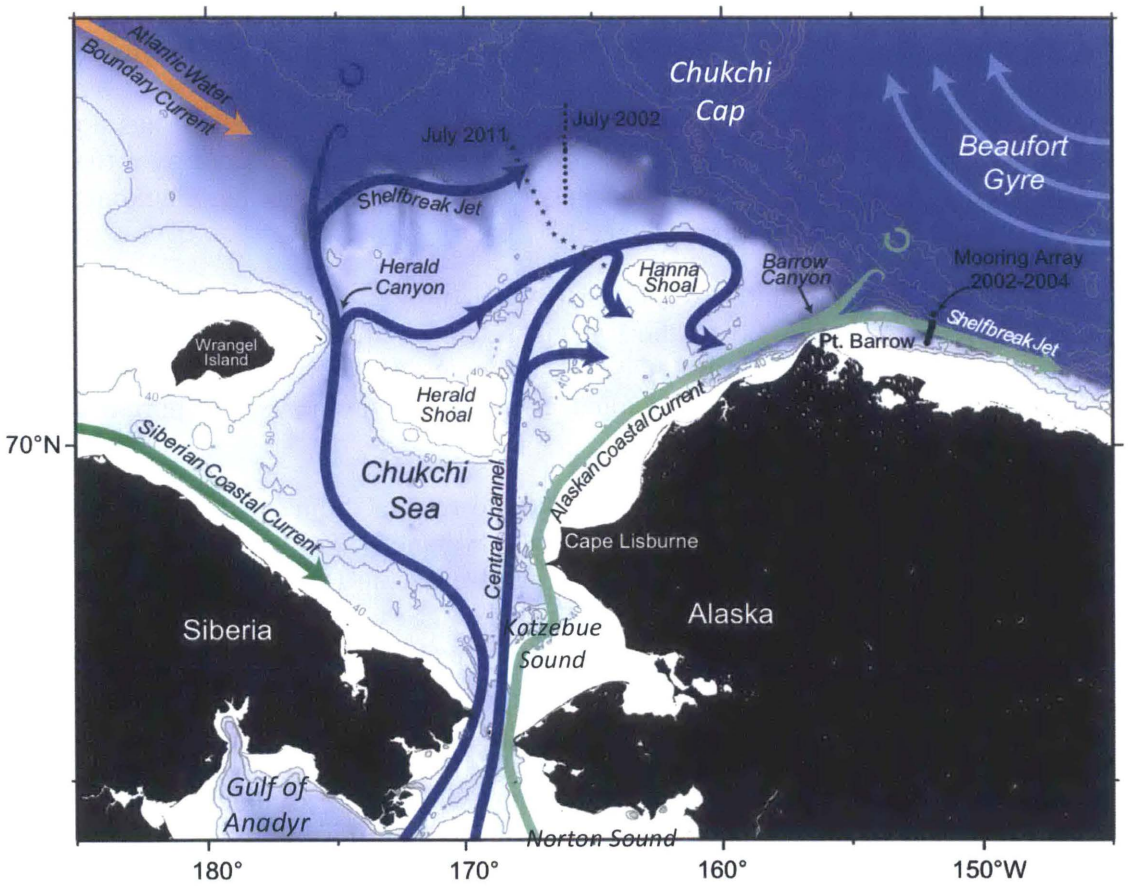

Figure 2-1: Mean circulation pattern of the Chukchi Sea. (Spall et al., 2014)

The annual mean transport through the Chukchi to the Arctic in 1990 and 1991 was estimated to be 0.8 Sv (Woodgate et al., 2005). The vast majority of this water moved through one of four pathways, Barrow Canyon, the Central Channel, Herald Canyon and De Long Strait (west of Wrangel Island). All four transports are on the order of 0.1-0.3 Sv. This mean transport is driven by sea surface height differences between the Pacific and the Arctic, but the scale of the weekly transport, variability must be considered. Consistent westerly and northwesterly winds lead to strong southward transport for periods when the wind speed is sufficient to drive currents that overwhelm the barotropic forcing from the south. Of the four pathways, Herald Canyon was the least susceptible to temporary wind driven reversals (Woodgate et al., 2005). The weekly transport can vary from a maximum of 2 Sv to the south to a maximum of 3 Sv to the north (Woodgate et al., 2005).

Residence time in the Chukchi Sea has been estimated to be between one and six months. The lowest values are expected in late summer and the highest values are expected in the late winter when conditions are the least variable and surface winds have the least effect on circulation (Woodgate et al., 2005). This counterintuitive result comes from the fact that the pressure gradient driven component of the northward flow is slow year round. The low residency times in the summer come from periods of strong wind driven northward flow. Even though these episodes are followed by strong wind driven southward flow, they are sufficient to significantly reduce the mean residency time in the summer (Woodgate et al., 2005). The high winter residency times allow for the temperature and salinity (T-S) stability of the Chukchi observed through these months (Woodgate et al., 2005). Residence time over Hanna Shoal has not been estimated separately, but the finer sediment of a more depositional nature found over the shoal suggests that residence time might be longer over the shoal than the surrounding Chukchi waters where gravel bottoms are common (Norcross et al., 2013).

The flow field over the Chukchi rapidly responds to wind forcing, demonstrating high spatial coherence over a basin scale. Motion in the sea takes the length scale of the wind forcing (Woodgate et al., 2005). This means instantaneous velocities through the water column will almost never resemble the mean pattern. This intense variability may be very important for the zooplankton communities in the Sea.

The scale and patterns in interannual variability are key to understanding data taken from any single year. Even as climate change gradually reduces the average size of the permanent ice cap, the extent and quality of winter ice cover remains highly variable (Day et al., 2013). Until recently, seasonal variation of ice cover over the Chukchi Sea was seen as the dominant environmental factor affecting total primary productivity (Wang et al., 2005), but now it is clear that annual primary productivity in areas that host under-ice blooms may have been underestimated by a factor of ten (Arrigo et al., 2014). In a series of 1-D Nutrient Phytoplankton Zooplankton Detritus and Bacteria (NPZD+B) model runs, ice cover and quality was found to have a very small impact on total annual primary productivity for the Chukchi (Palmer et al., 2014). Nutrient supply via upwelling had a much more significant effect on total annual primary productivity for the Chukchi (Spall et al., 2014).

Over the course of the summer, warm, moderately saline Bering Sea Summer Water replaces the cool, fresher melt waters from the spring at the surface and the cold saline, Chukchi Sea formed Winter Water at depth (Weingartner et al., 2013). The convergence of Bering Sea Summer Water from the west and winter water over an area just south of Hanna shoal leads to large

horizontal gradients in water properties over scales ranging from 50-100 km that propagate east from Central Channel over the course of the summer. These gradients affect shelfwide stratification and lead to ocean heat flux convergence supplanting solar heating in September (Weingartner et al., 2013).

The exact route followed by the Bering Sea Water arriving in the Chukchi is variable from year to year, and certain areas might not see any in a given year. In 2008-2010 the complex late summer distributions of water properties did not appear to be linked with these large interannual differences in shelfwide ice retreat. They appeared to be controlled much more by regional winds and processes occurring in the Bering Sea after the disappearance of the ice (Weingartner et al., 2013). In contrast, the variability in the water mass interactions seems to drive much of the interannual variation in zooplankton populations (Day et al., 2013)

In stark contrast to the very complicated situation present in the summer, the entire Chukchi collapses into a very small T-S region close to the freezing point over the winter. This indicates that the processes of brine rejection and storm mixing dominate over the advection in determining the properties of the region (Woodgate et al., 2005). This is reinforced by the longer winter residence times, giving the shallow sea plenty of time to homogenize. When early spring arrives, the Chukchi is characterized by very high nutrient concentrations, but low irradiance as a consequence of both sea ice cover and short daylight hour durations limiting phytoplankton growth (Hill et al., 2005).

In general, seasonal variability is much greater southeast of Hanna Shoal where warm, fresh waters from the coastally trapped Alaska Coastal Current (ACC) enter the eastern Chukchi than to the west, where the seasonally present Siberian Coastal Current dominates. The Siberian Coastal Current supplies fresh, cold water and exhibits a flow field that is much less linked to local wind patterns (Woodgate et al., 2005). Runs of a hydrostatic version of the MIT primitive equation circulation model (Spall, 2007) and the Regional Ocean Model System (ROMS) (Winsor and Chapman, 2004) predict that the mean flow will be clockwise around Hanna Shoal itself. This would cause remnant Winter Water to be advected to the southwest. Limited observations from 2008 to 2010 supported this prediction (Weingartner et al., 2013).

The northern boundary of Hanna Shoal is roughly aligned with the shelfbreak separating the Canada Basin from the shallow Chukchi Sea shelf. The southern portion of the Beaufort Gyre flows parallel to the break from East to West (Figure 2-1). The shelfbreak jet to the south of the gyre has two primary modes. The first is a surface intensified jet moving warm, buoyant Alaska Coastal Water (ACW) east in the late summer. This process leads to both baroclinic and barotropic instability resulting in the propagation of warm core eddies into the Southern Beaufort. The second is a bottom-intensified current that advects weakly stratified Chukchi summer water east (Nikolopoulos et al., 2009). This process is baroclinically unstable to mid depth and can result in warm core eddies that reach the interior basin (Pickart et al., 2005). The first state is much stronger; it spins down 300 km offshore and extends up to 1400 km, sometimes to the Canadian Archipelago. The second state is weaker; it spins down 150 km offshore and does not extend far into the Beaufort Sea (Von Appen and Pickart, 2012). In 2002, significant quantities of particles and zooplankton were found in Barrow Canyon traveling to the northeast, but theoretical sinking rates imply that most of this material entered the benthos before the water carrying it left the shelf (Ashjian et al., 2005). The only significant observed off-shelf fluxes of plankton and particles from the Chukchi (including Hanna Shoal) to the Arctic Basin were in

eddies located off the Beaufort Shelf surveyed in 2004 (Ashjian et al., 2005; Llinás et al., 2009). These cold-core features with eight-kilometer radii were found to contain North Pacific water and copepods in the center, but the outer portion hosted numerous Arctic copepods. It is believed that as the eddies formed and traveled north they entrained significant quantities of shelf waters. It is thought that this is the primary mode by which biomass is exported off the shelf into the nutrient poor central Arctic (Llinás et al., 2009).

The overall importance of this advective regime is most easily seen when the Chukchi Sea is compared with the Barents Sea. The water entering the Chukchi from the Bering is prechilled, whereas the water entering the Barents from the Norwegian Sea is warmed by the North Atlantic Drift (Hunt et al., 2013). This difference in heat content results in massive biological contrasts in spite of the many physical similarities between the two seas. Both are found at similar latitudes, host similar durations of seasonal ice coverage, and are Arctic shelf seas home to northward flowing mean currents. Yet the Barents Sea hosts very high annual primary productivity and a vibrant fish community, both of which the Chukchi Sea lacks (Hunt et al., 2013).

2.2 Primary Production Patterns

In general, lower trophic dynamics in the Bering and Chukchi Seas are highly complex due to the manner in which biophysical interactions occur at different spatial and temporal scales (Wang et al., 2005). In July and August 2002 the average primary productivity of shelf waters less than 220 meters deep was 709 $mgC/m^2/day$. These two months accounted for 45% of the annual total of 97.4 $gC/m^2/year$ (Walsh et al., 2005).

Phytoplankton pigmentation and size fractionated biomass both showed significant spatial and temporal variation during the spring and summer of 2002 (Hill et al., 2005). In the spring of 2002, the Chukchi's phytoplankton community was dominated by 5 μm and larger haptophytes/diatoms while the slope and Arctic basin's phytoplankton community was dominated by 5 μm and smaller prasinophytes and cholorophytes with high concentrations of chlorophyll b. In the summer, small prasinophytes and large haptophytes/diatoms co-dominated the near surface assemblages that were nitrate depleted over the shelf, slope and basin. The upper nutricline could be found at 1-15% surface irradiance, and here the large diatoms alone dominated. The consistency of the assemblages across the shelf break was explained by advection off the shelf through Barrow Canyon (Hill et al., 2005).

Wang et al. (2005) found that an abnormally early retreat of sea ice through the Chukchi, such as the one witnessed in 1998 following an intense El Niño, resulted in a correspondingly early and massive spring phytoplankton bloom. From 1998-2002 the chlorophyll concentration was found to increase from a nominal amount in April to a maximum in mid-spring in the southern Chukchi and a maximum in mid-summer in the northern Chukchi. In general, the spring blooms were largest in the southwest Chukchi and most persistent just north of Bering Strait. This is ascribed primarily to the influx of nutrient rich Anadyr Water (Wang et al., 2005).

From 1998-2002, the strength of the negative correlation between chlorophyll concentration and ice extent was greatest in May and the strength of the negative correlation between temperature and ice extent was greatest in April (Wang et al., 2005). This suggests that a particularly warm April should lead to a particularly quick ice retreat and a particularly strong bloom in May,

whereas a particularly warm May for example would not have as strong an effect on chlorophyll production through the summer.

Picophytoplankton are incredibly important worldwide. In oligotrophic waters they dominate biomass and possibly primary productivity while in temperate and subpolar waters they still dominate biomass (Lee et al., 2013). In the Chukchi in 2009, *Prochlorococus* and *Synechococcus*, two key members of the picophytoplankton, were found to make up 30% of the phytoplankton smaller than 20 um with concentrations of 295 cells /ml and 590 cells/ml respectively. The balance of this size fraction was made up of pico- and nanoeukaryotes (Lee et., al 2013). These samples were taken in open water. In the 2011 under ice bloom picophytoplankton was found to only make up 1% of the phytoplankton biomass; diatoms made up 87%. Outside of bloom conditions diatoms were less abundant, but they almost always represented at least a plurality of phytoplankton biomass in the Chukchi (Laney and Sosik, 2014).

Recent work has shown that under ice blooms before ice retreat are of the same order of magnitude and sometimes larger than the bloom in the retreating marginal ice zone. Their spatial extent from 1998-2012 was 2.5 times the spatial extent of the bloom in the marginal ice zone (Lowry et al., 2014). But even if variation in ice cover appears only to have a small influence on total primary productivity of the Chukchi, the bloom features are indeed controlled by the interannual variability in ice cover. In a light ice year, the spring retreat is quick, leading to pelagic and ice edge blooms. In a heavy ice year, the spring retreat is much slower, typically leading to more important under and within ice blooms (Day et al., 2013). Lowry et al. (2014) also found consistent spatial patterns in the relative importance of these features. Under ice blooms tend to dominate in the west whereas marginal ice zone blooms tend to dominate in the south and east.

The timing and intensity of primary productivity in the Chukchi Sea is controlled by light intensity and the concentration of nutrients much more than ice cover properties. Until recently it was assumed that ice needed to retreat for any meaningful primary productivity to take place. It is now believed that once 10% of the surface of the ice is covered by melt pools that there is enough light to support shade adapted phytoplankton below the ice. An increase in melt pools to cover 20% of the surface further increases net primary production by 26%, but further presence of melt pools has little effect on net primary production (Palmer et al., 2014). These under ice blooms have the potential to deplete the local nutrient concentration, so marginal ice blooms only take place in water masses that did not host significant under ice blooms (Palmer et al., 2014). The interannual variability in the concentration of nutrients is the primary variable that drives interannual variability in total primary production. The concentration of nutrients available in a given spring/summer appears to be mainly driven by the extent of upwelling along the shelf break. It is important to realize that wind driven upwelling has been observed even when the region hosts 100% ice cover (Pickart et al., 2013; Spall et al., 2014). Persistent, strong east winds during the late spring and summer of 2011 resulted in massive upwelling supplying nutrient rich water from the bottom boundary layer of the slope to the central Chukchi. In 2002, the lack of this atmospheric phenomenon meant lower nutrient concentrations throughout the Chukchi and much lower annual total primary production throughout the system (Spall et al., 2014).

2.3 Zooplankton Community

Hopcroft et al. (2010) identified six distinct zooplankton communities in the Chukchi in 2004, each associated with a specific water mass (Figure 2-2): Euryhaline species in the warm, fresh waters of the ACC (red), Bering Sea shelf species in cool, salty Bering Sea Water (BSW) (cyan), Bering Sea oceanic species in cool, salty BSW (blue), a transitional group with members from the second and third communities (magenta), Neritic Bering Sea species in cold, salty Bering Winter Water (BWW) (grey), and Arctic Shelf species in cold, fresh resident Chukchi water (green) (2010).

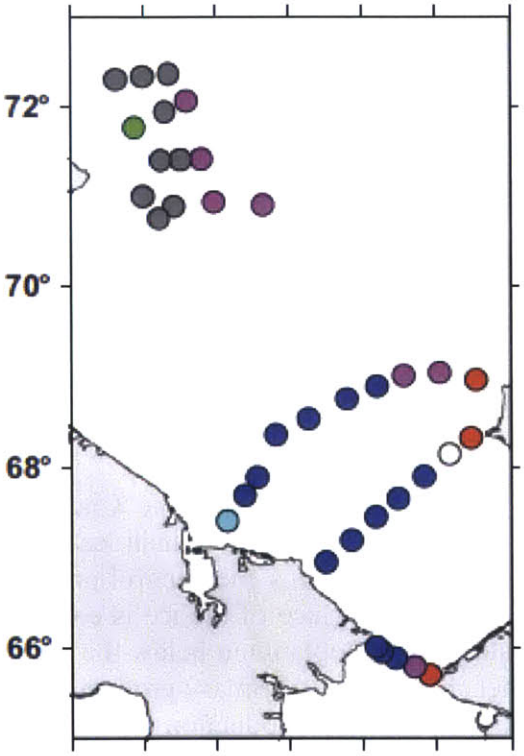

Figure 2-2: Spatial distribution of zooplankton communities in the Chukchi Sea. (Hopcroft et al. 2010)

Like the phytoplankton community, the zooplankton community is highly seasonal in nature, typically following a pattern with a single peak in abundance each year. The vertical distribution is also seasonal. Sampling of the biomass dominant copepods of the genus *Calanus* from an ice station found that biomass over the Chukchi Plateau in summer 1998 was much higher than the biomass over the Arctic Basin in fall 1997 and winter 1997-1998 (Ashjian et al., 2003). The biomass maximum during most of the year was found between 200 and 1500 meters, but during summer the maximum was found in the top 200 meters. This follows the generally accepted theory that *Calanus* spp. copepods, the dominant zooplankton, spend their winters at depth in diapause and their summers as active grazers and predators near the surface.

Three sites studied from 2008-2010 during the Chukchi Sea Environmental Studies Program (Figure 2-3) were found to form a pelagic-benthic continuum in terms of their zooplankton community composition (Questel et al., 2013). Klondike, the southernmost site, was on the border of the Central channel. It was dominated by pelagic species. Burger, northeast of Klondike, was directly south of Hanna Shoal. It was dominated by benthic species. Statoil, northwest of Burger, was located on the west-southwest portion of Hanna Shoal and also bordered the Central Channel. It hosted similar abundances of pelagic and benthic species (Day et al., 2013).

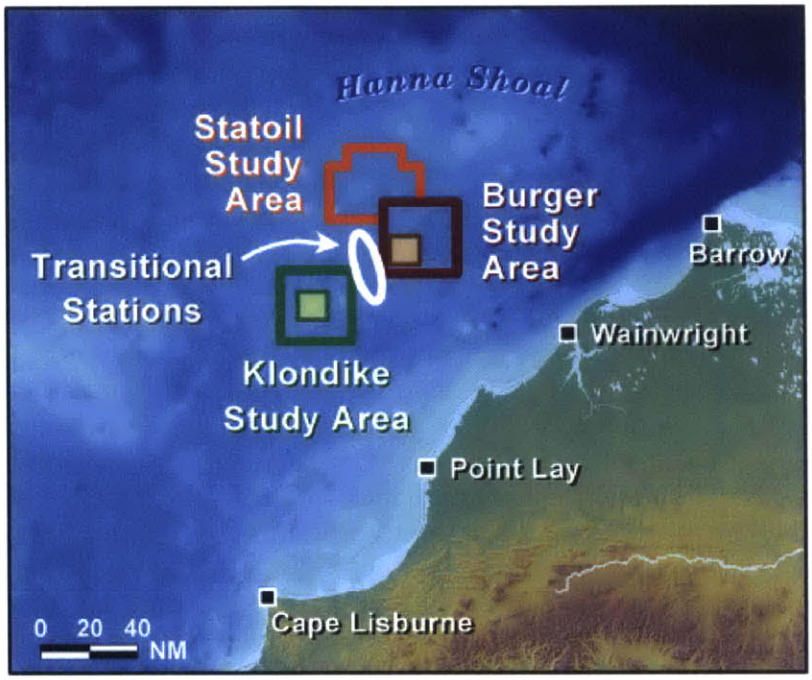

Figure 2-3: Location of 2008-2010 study sites. (Day et al., 2013)

In line with this continuum, Klondike was found to have low benthic diversity and biomass, high oceanic zooplankton biomass along with more fish and many planktivorous birds. Burger was found to have a denser benthic community with higher biomass along with high neritic zooplankton biomass and many benthic feeding marine mammals (Day et al., 2013).

The four usual *Calanus* species in the Arctic include two endemics: *C. glacialis* and *hyperboreus* and two expatriates: *C. finmarchicus* and *C. marshallae*, the most common *Calanus* species in the north Atlantic and north Pacific respectively (Hopcroft et al., 2010; Ji et al., 2012). *C. glacialis* will be discussed at length below. *C. glacialis*, which dominates north of the Bering Strait and *C. marshallae*, which dominates south of the Bering Strait, cannot reliably be distinguished from each other visually due to similarities in size, pigmentation and overall appearance. Unless genetic work is done, these species are generally considered together with the understanding that north of the Strait, the species complex is expected to have many more *C. glacialis* and vice-versa south of the Strait (Plourde et al., 2005). Throughout this document references to *C. glacialis* would most properly be made to the *C. glacialis and C. marshallae* species complex, however for simplicity and because in our area of interest the complex is dominated by *C. glacialis* we will refer to the complex simply as *C. glacialis*.

Zooplankton abundance in the Chukchi is highly variable, both temporally and spatially. Considering the summers of 1991, 1992, 2007 and 2008, zooplankton abundance in the Chukchi Sea ranged from 4,000 ind/m^2 to 316,000 ind/m^2 with a mean of 70,000 ind/m^2 (Matsuno et al., 2011). Likewise, the biomass varied from .07 g wet mass/m^2 to 286 g wet mass/m^2 with a mean of 36 g wet mass/m^2 (Matsuno et al., 2011). This variability means that any attempt to find general patterns in distribution must incorporate at least two years of data, preferably more.

In general, zooplankton aggregations are expected above key bathymetric features such as seamounts, canyons and shelf breaks (Genin, 2004). Bathymetrically forced upwelling drives these persistent concentrations over large features where the residence time of upwelled water is of sufficient duration to enhance primary production (Genin, 2004). Daily accumulations of zooplankton occur where individuals swim against downwelling or upwelling to maintain their preferred depth (Genin, 2004). Topographic blocking is another concentration pathway; zooplankton are advected over shallow water at night and cannot descend to depth during the day (Genin, 2004). This may be significant in the Chukchi in the spring and fall, but the lack of night in the early summer changes the dynamic dramatically.

In mid to late summer 2002, the most common taxa observed by a video plankton recorder (VPR) around the Chukchi shelf break were copepods, diatom chains, decaying diatoms, marine snow and radiolarians (Ashjian et al., 2005). Vertical distributions of zooplankton around the shelf break were observed to closely follow the physical structure of the water column and thus sharp discontinuities in abundance of all categories were seen at the shelf break (Ashjian et al., 2005). As noted during the physical description of the Chukchi, the dominant transport occurring at the shelfbreak itself is east and not north into the basin. In 2002, as expected, it appeared that zooplankton were being advected east along the break in the observed currents (Ashjian et al., 2005).

In August 2004, seven transects across Herald Canyon, well to the west of Hanna Shoal, yielded 50 species of holoplankton including 23 different copepods along with many species of meroplankton (Hopcroft et al., 2010). Barnacle and echinoderm larvae dominated the meroplankton numerically. Copepods made up over 70% of the holoplankton biomass and over 88% of the holoplankton abundance, which represented over 60% of the total plankton abundance. The copepods were numerically dominated by six small species, but *C. glacialis* and two species of *Neocalanus* each equaled or exceeded the biomass of the six small copepods. The most abundant noncopepod holoplankter in terms of both abundance and biomass was the larvacean *Oikopleura vanhoeffeni.* The primary copepod predators identified were chaetognaths and a diverse assemblage of cnidarians (Hopcroft et al., 2010).

In 2008-2010, Questel et al. (2013) sampled three sites roughly 200 nm to the east of Herald Canyon (Fig. 2.3.3) and found 69 species of holoplankton including 25 species of copepod. All were typical for the region and many appeared to be seeded from the Bering Sea. Abundances found to be both lower and higher than the numbers reported by Hopcroft et al. (2010) for Harold Canyon. In 2008 they reported 68% of the Hopcroft et al. number and in 2010 they reported 211% of the Hopcroft et al. number. Biomass ranged from 25% of the Hopcroft et al. number in 2008 to 245% of the Hopcroft et al. number in 2010. The majority of the increases came from more lipid rich copepods such as *Calanus* spp. being present in 2010. Meroplankton abundance ranged from 26% of the Hopcroft et. al number in 2009 to 417% of the Hopcroft et al. number in

2010 (Questel et al., 2013). These differences highlight the scale of the interannual variability in both the holo- and meroplankton communities.

The physical differences described earlier between water entering the Barents Sea and the Chukchi Sea are matched by their biological differences. Water entering from the Norwegian Sea is filled with lipid rich zooplankton whereas such zooplankton are much less abundant in water entering from the Bering Sea. Since the primary productivity in both bodies is roughly equal, this advection explains how the Barents is able to support a vast commercial fishery, which does not exist in the Chukchi. (It has an order of magnitude less fish biomass than the Barents Sea (Hunt et al., 2013).) The presence of healthy fish populations in the Barents supports twice the density of cetaceans and nesting seabirds relative to the Chukchi, whereas the tight pelagic-benthic coupling in the shallow Chukchi supports a thriving benthic community and twice the density of benthic feeding pinnipeds (Hunt et al., 2013). Not only are fish rare in the Chukchi, most are incredibly small. When fish communities of the three sites in the northeastern Chukchi (Figure 2-3) were compared in the summers of 2009 and 2010, the only conserved ecological quantity was the fact that the populations were always dominated by individuals less than 150 mm total length (Norcross et al., 2013). The zooplankton community and the harsh physical environment in the Chukchi are the driving factors behind this.

2.4 *Calanus glacialis*

C. glacialis is a typical panarctic shelf species. It is common in the Barents Sea north of the polar front, on the East Greenland Shelf, in the Canadian Archipelago, in Baffin Bay, in the Chukchi Sea, in the White Sea and on the Siberian Shelf as far to the east as the Sea of Okhotsk (Falk-Petersen et al., 2009). Despite being an omnivore with an observed preference for microzooplankton (Campbell et al., 2009), *C. glacialis* is one of the three most important grazers of phytoplankton and ice algae in Arctic Seas. They play a particularly key role in the lipid based energy flux by converting low energy carbohydrates and proteins found in ice algae and phytoplankton into high energy wax esters (Falk-Petersen et al., 2009).

During a 1997-1998 ice station whose sampling spanned both the Arctic Basin and the Chukchi Cap, no consistent temporal or regional patterns in *C. glacialis* condition and body size were identified (Ashjian et al., 2003). However, the population age structures observed indicated that both *C. glacialis* and *C. hyperboreus* were reproducing in the Arctic Basin. These findings contrast with observations by Falk-Petersen et al. (2009) that *C. glacialis* spawning is constrained to the shelf, slope and fjords. At times, the abundance of *C. glacialis* in the basin dropped so low that it appeared to not be self-sustaining in the Basin (Ashjian et al., 2003). The biogeography of *C. glacialis* in the Arctic is likely a function of life history traits interacting with a harsh, highly seasonal physical environment (Ji et al., 2012).

C. glacialis has a full natural life span of 1-3 years depending on the population's home range (Falk-Petersen et al., 2009). *C. glacialis* in the Bering Strait is believed to live 2-3 years. Typically, individuals spawn during the spring/early summer of their second or third year. By the end of the first summer individuals must advance to the copopodite IV stage and build up sufficient lipid reserves to survive the winter. During the second summer they typically advance to copopodite V stage. They often only reach full maturity just before spawning. This life history also can be accomplished in less than 3 years (Daase et al., 2013). Gonads are typically

developed to an advanced stage using lipid reserves during the second winter. The impetus to spawn varies geographically (Falk-Petersen et al., 2009).

C. glacialis has demonstrated the ability to follow distinct reproductive strategies depending on their environment. It commonly exhibits pulsed reproduction with overlapping cohorts present together as a result of ontogenetic redistribution (Ashjian et al., 2003). South of Spitsbergen, *C. glacialis* acted as a capital breeder, spawning early before the spring bloom supplied parents with food (Daase et al., 2013). This allowed the new generation to sync their growth and development with the phytoplankton bloom. In the Canadian Arctic, *C. glacialis* were seen to use the initial under ice algae bloom to fuel spawning. This allowed the growth and development of their offspring to be supported by the secondary phytoplankton bloom in the water column (Daase et al., 2013).

The intense seasonality of the Arctic environment makes the life strategy of going into a dormant state during the less productive periods critical for the survival of organisms that live for more than one growing season. In copepods, this state is called diapause and involves descending to depth, minimizing metabolic needs by reducing movement and sensory responses, and surviving off lipid reserves built up during the summer and early fall. *C. glacialis* diapauses between 200-300m, normally in the Canadian Archipelago or the Arctic Basin itself (Falk-Petersen et al., 2009).

Diatom fatty acid trophic markers dominated in *C. glacialis* lipids sampled in the Barents Sea, emphasizing the importance of diatoms in controlling populations of the copepod over other food sources such as dinoflagelates and *Phaeocystis spp.* (Falk-Petersen et al., 2009). Since diatoms dominate the phytoplankton community over the entire Chukchi in the spring and summer (Balch et al., 2014), this likely plays into the success of *C. glacialis* in the region. It is important to note that a substantial portion of *C. glacialis'* diatom originated lipids comes from secondary consumption. Microzooplankton, including naked ciliates and heterotrophic gymnodinoid dinoflagelates, are the preferred food of *C. glacialis* and many other mesozooplankton (Campbell et al., 2009). Microzooplankton have been observed consuming diatoms (Sherr et al., 2013) and in the Chukchi they were found to contribute approximately 50% of the total grazing effort on phytoplankton. Both micro- and meso- zooplankton each only consumed about 22% of the total primary production in the Chukchi (Campbell et al., 2009). Within the 2011 under-ice bloom observed in the northern Chukchi Sea, bacterial biomass was only 3.5% that of the phytoplankton (Ortega-Retuerta et al., 2014); such a small number of bacteria could not consume much of the 56% of primary production not eaten by the zooplankton. This means more than half the primary production is exported to the benthos or out of the Chukchi.

2.5 Ecosystem Modeling

A Nutrient, Phytoplankton, Zooplankton, Detritus (NPZD) ecosystem model linked to an ice and ocean physical model was able to reproduce the general seasonal cycle observed for 2007-2008 (Wang et al., 2013). Specifically it was able to match the structure of in situ observations taken over the Chukchi Shelf in August 2007 and over the Bering Shelf in July 2008 (Wang et al. 2013). The work included a sensitivity experiment to see how changes in forcing might affect the timing and intensity of the phytoplankton bloom in the Bering and Chukchi Seas. A 10% increase in solar radiation was found to have no effect on either the timing or the intensity of the bloom. A 20% increase in nutrient loading increased the intensity of the bloom by 7% with the

largest gains seen over the slope. A 2°C increase in temperature led to an 11% increase in the intensity of the bloom, indicating that in fact the extreme low temperatures present in the environment slow growth more than light or nutrients (Wang et al., 2013).

Walsh et al. (2005) used a three-dimensional circulation model linked to an ecological model to investigate carbon and nitrogen cycling in the Chukchi and Beaufort Seas in 2002. They found that the seasonal penetration of Anadyr water matched shipboard observations, as did the nitrate, silicate, dissolved inorganic carbon, chlorophyll a, dissolved organic carbon, and ammonium distributions. These approaches show promise for using complex models in the region, but it is important to always remember that model output matching observations does not imply that the model accurately captures the mechanism through which the observed values came about.

2.6 The Finite Volume Community Ocean Model (FVCOM)

The FVCOM was originally developed by Chen, Liu and Beardsley and was first published in 2003 (Chen et al., 2013a). Since then it has been continually improved and used for numerous applications across many oceanographic disciplines. It is a three dimensional prognostic model driven by tidal, river, atmospheric and ice forcing. Its characteristic unstructured grid of finite volumes allows it to use a numerical approach when dealing with complex coastal geometry, and thus yield more realistic results than many competing models. It solves the governing equations on Cartesian or spherical coordinates in integral form by computing the fluxes between non-overlapping horizontal triangular control volumes. As such the model is conservative both locally and globally. FVCOM is able to leverage Finite-Elements Methods for geometric flexibility and Finite-Differences Methods for simplicity and computing speed. It began as a physical ocean model, but is now a fully coupled ice, ocean, wave, sediment, and ecosystem model (Chen et al., 2013a).

2.7 Individual Based Model (IBM)

An IBM, also known as an Agent Based Model, is a model that represents a system's individual components and their behaviors instead of using variables to represent the state of the system as a whole. Agents are unique and interact with their neighbors and their local environment. Environmental variables are allowed to vary over time and space. This architecture allows us to look at what happens to a system due to individuals and what happens to individuals due to the system, which in turn permits us to study emergence, the system dynamics that arise from these interactions (Railsback and Grimm, 2012).

IBM's can be used for a considerable number of applications, but here we will focus on their use in answering questions related to plankton ecology. In this case, IBM's are coupled to a physical model that provides realistic current and temperature fields that are used by the IBM to move individual planktors and determine such states as development rate and fitness. Miller et al. (1998) developed an IBM to track *C. finmarchicus* over the Gulf of Maine coupled with the Dartmouth Model of New England Regional Circulation in an effort to identify sources and sinks of the two generations of copepods that mature during the growing season. Follow on work by Gentleman et al. (2008) and Neuheimer et al. (2010a) focused on the inclusion of a stochastic "fitness" parameter that determined an individual copepod's ability to reproduce, develop and survive. They experimented with "fitness" parameters that were prescribed a priori (genetic predisposition) and those that were solved dynamically from history, condition or environment.

They found the approach provided considerable power for quantitative hypothesis testing. Looking at populations originating off the coast of Nova Scotia, Neuheimer et al. (2010b) found that temperature has a dominant effect on development and egg production and that egg recruitment was affected by both temperature and the abundance of females. They also determined that the parameterized mortality rate had a strong influence on abundance, so they argued that environmentally dependent mortality rates are needed to get results consistent with observations.

The Finite Volume Community Ocean Model I-State Configuration Model (FISCM) follows the fate of agents as they are advected through an environment by currents calculated by a physical ocean model, specifically FVCOM. It uses a fourth order Runge-Kutta time marching scheme to very accurately track particles at a variety of time steps. Agents can be simple particles or they can represent biological units and develop or exhibit behaviors based on the presence or absence of cues such as food or temperature levels. This model was used to investigate the global distribution patterns of four key Arctic copepods (Ji et al., 2012). The IBM showed that *C. marshallae* and *C. finmarchicus,* the two expatriate species, were unable to penetrate, survive and colonize the Arctic Ocean under present conditions for two main reasons. First, they had insufficient time in food rich and/or warm environments to develop and build up lipids prior to the cessation of food availability in the fall, which prompted them to enter diapause. Second, transport north was generally very slow; successful individuals were able to develop relatively quickly in the south and never entered the Arctic in significant numbers (Ji et al., 2012).

The same model run suggested that the persistence of *C. glacialis* and *C. hyperboreus* in northern ranges that were not suitable for *C. marshallae* and *C. finmarchicus* was mainly due to three factors. First, the Arctic endemics have faster development rates at low temperatures, second, they are able to enter diapause at an earlier developmental state and third, they are able to feed on ice algae, which the southern expatriates may not be able to do (Ji et al., 2012). The model also found that even *C. glacialis* and *C. hyperboreus* were unable to develop enough to successfully enter diapause in the central Arctic. This implies that the second and third year populations found in the central Arctic must have been advected from the surrounding regions (Ji et al., 2012).

2.8 Climate Change Impacts

Sea ice cover in the western Arctic during the summer has decreased drastically in the last two decades due to an overall increase in surface temperatures (Sedláček et al., 2012). Zhang et al. (2010) ran a coupled biophysical model consisting of three model elements: a sea ice model, an ocean circulation model, and a pelagic biological model for the period of 1988-2007, chosen due to the decrease in mean sea ice cover observed over these years. Photosythetically Active Radiation (PAR) and primary productivity increased by almost 50% over the 20 years due to both increased mean open water and decreased mean ice thickness. PAR and primary productivity did not change in areas that were not ice covered in 1988. The general increase in primary productivity was also linked to increases in both phytoplankton and zooplankton biomass (Zhang et al., 2010). A key mechanism here is that the decline of sea ice increases air-sea momentum transfer, leading to more upwelling and mixing, and thus increased nutrient availability in the euphotic zone and finally in turn, more primary productivity (Zhang et al., 2010). The importance of interannual variation in the face of this current warming trend must

always be considered. Sea ice retreat was early and temperatures warm in 2009 compared to 2008, but 2010 fell between the two (Questel et al., 2013). Modeling a consistently decline ice cover in the Western Arctic would yield very unrealistic results. Also, the importance of Ekman dynamics in a fully ice covered sea are only now being understood (Spall et al., 2014). It is possible that the Zhang et al. (2010) model overestimates gains in primary productivity by overstating the increase in air-sea momentum transfer following loss of ice cover.

Ji et al. (2012) also used their IBM to look at the effects of a 2°C increase in mean water temperature and found that of the four key species of Arctic copepod, the two natives would be able to increase their range further north, but that the two expatriates would still be unable to further penetrate the Arctic due to the short duration of the growing season and the need to acquire enough lipid reserve before entering diapause.

The greater abundance and biomass of zooplankton in the Chukchi during 2007 and 2008 compared to 1991 and 1992 suggests that decreasing ice cover is driving an increase in zooplankton production (Matsuno et al., 2010). Matsuno et al. split the Chukchi zooplankton community into four clusters based on species makeup. The center of each of the four clusters' distributions was further north in 2007 and 2008 compared to its position in 1991 and 1992 (2010). This movement seemed to suggest that Arctic species were being replaced by Pacific species (Matsuno et al., 2010). However, in general, total annual primary production appeared to be nutrient limited in the Chukchi, suggesting that without significant eutrophication, less ice cover will not lead to vastly increased primary productivity in the region (Walsh et al., 2005).

This implies that further increases in secondary production in the zooplankton community would also be unlikely without eutrophication. That said, Lee et al. (2013) projected that temperature and ammonium concentrations will increase in the Chukchi Sea in the future regardless of eutrophication. They found both to be positively correlated with abundance of total phytoplankton, particularly the <20 um size fraction. Such an increase would likely lead to higher productivity (Lee et al., 2013). This simply shows that the system is complex and it remains to be seen what the net result of warming will be for primary and secondary production in the Chukchi.

Hunt et al. (2013) looked at a generalized warming scenario for both the Barents and Chukchi Seas. In such a scenario, the southern Barents would likely remain ice free year round leading to an increase in productivity at all trophic levels throughout the Sea. In contrast, the shallow nature of the Chukchi Sea and the continued introduction of relatively prechilled water from the Bering would lead it to continue to freeze completely in the winter. Even in this warming scenario, the well-mixed water column in the northern Bering Sea and Chukchi would be below zero for about eight months of the year. Fish lacking adaptations for sub-zero temperatures are unlikely to thrive, as they would not have the temperature refuge they have in the Barents. In addition, the persistent cold temperatures of the Chukchi Sea would continue to slow the feeding and growth of zooplankton and fish (Hunt et al., 2013). Thus the strong benthic coupling would be expected to continue, even in such a generalized warming scenario.

2.9 Moving Forward

Clearly much progress has been made in recent decades towards understanding the dynamic environment of the western Arctic and the planktonic biota it hosts. At the same time, the

pathways these biota take as they move from source regions to sink regions remain poorly understood. Here we use an individual based model to advect observed distributions of a key Arctic copepod (*C. glacialis*) both forward and backward in time to investigate the locations of these regions and the physical oceanographic features that are key in transporting these copepods from source to sink.

Chapter 3

Methods

3.1 AO-FVCOM Output

In June 2014, the Marine Ecosystem Dynamics Modeling Laboratory at the University of Massachusetts Dartmouth provided output from the newest version of the AO-FVCOM that encompasses 61°N to 77°N and is pan Arctic. Files for each month from August 2011 through December 2013 were provided in Network Common Data Format (NetCDF) with daily mean values for numerous variables, some as element averages at the center of the edges of the triangular control volumes and others as control volume averages stored at the central node of each control volume (Table 3.1.1).

Table 3.1 AO-FVCOM Output Variables

Variable	Edge or Volume	Units
Depth	Volume	Meters
Latitude	Volume	Degrees
Longitude	Volume	Degrees
Latitude	Edge	Degrees
Longitude	Edge	Degrees
Omega	Volume	s^{-1}
Sigma Layer	Volume	Proportion of Depth
Sigma Level	Volume	Proportion of Depth
Eastward Velocity	Edge	$m*s^{-1}$
Vertically Averaged Eastward Velocity	Edge	$m*s^{-1}$
Northward Velocity	Edge	$m*s^{-1}$
Vertically Averaged Northward Velocity	Edge	$m*s^{-1}$
Upward Water Velocity	Edge	m*s-1
Surface Elevation	Volume	Meters
Surface Ice Cover	Volume	Proportion of Cover
Turbulent Eddy Viscosity for Scalars	Volume	m^2*s^{-1}
Turbulent Eddy Viscosity for Momentum	Volume	m^2*s^{-1}
Salinity	Volume	psu
Temperature	Volume	deg C
Eastward Ice Velocity	Edge	$m*s^{-1}$
Westward Ice Velocity	Edge	$m*s^{-1}$
Ice Thickness	Volume	Meters

The output consists of 43,832 control volumes (Figure 3-1), including 8,032 in the area of interest defined as 63°N to 78°N and 179°W to 121°W (Figure 3-2). Within this subset of the model output, the average horizontal resolution is 21.7 km and each control volume contains an average area of approximately 218 km^2. As this is an unstructured grid, the horizontal resolution varied between 5.1 km in the Bering Strait and 61.1 km in the central Chukchi. In this realization, approximately 200 control volumes represent Hanna Shoal (Figure 3-2).

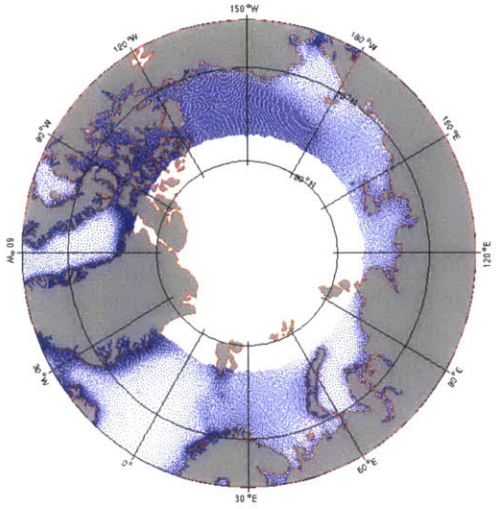

Figure 3-1: Central nodes for AO-FVCOM output.

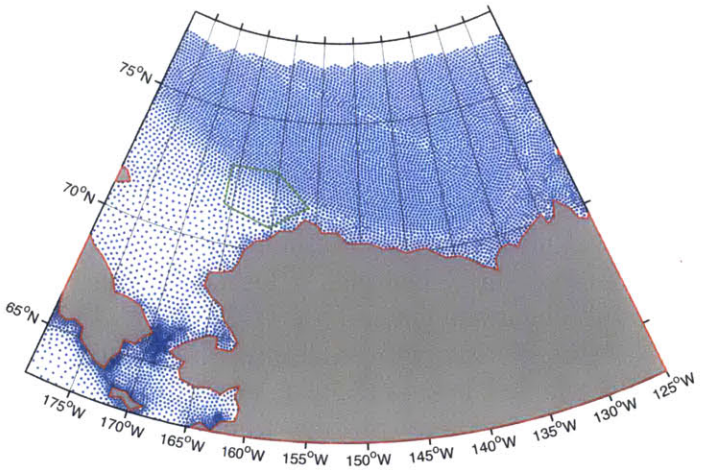

Figure 3-2: Central nodes of AO-FVCOM in the area of interest. The green box represents Hanna Shoal.

The model uses a hybrid terrain following coordinate. This means the vertical resolution varies based on the modeled depth at the center of each control volume. The water column is split into 45 sigma layers, which can be converted to depths by multiplying by the depth of the seafloor. In depths less than 225 m, the water column is split evenly between the layers. In depths greater than 225 m, the top ten and bottom three layers each represent 5 meters. The other 32 layers are evenly distributed through the remainder of the water column. Within the area of interest (Figure 3-2), vertical resolution varies between 11 cm and 118 m. Most of the Chukchi Sea is represented with a vertical resolution of less than 2 meters.

The AO-FVCOM is operated as a nested model within the global FVCOM. The resolution within the global FVCOM is significantly reduced, as its role is simply to provide realistic boundary conditions at the southern extent of the AO-FVCOM grid. This realization of the nested model system is a hindcast, meaning that it was run only after forcing data was observed and input into the model. The output used here includes the last three years of output generated during a 36-year model run.

The merged global-AO FVCOM was initialized by running it for 50 years under climatologic meteorological forcing and river discharge. In 1978 observed forcing replaced the climatological forcing and output was collected through 2013. This observed forcing captured the impact of tides, river discharge, surface heating, net surface precipitation, surface winds, and atmospheric pressure gradients.

The astronomical tidal forcing included the S_2, M_2, N_2, K_1, O_1, P_1, Q_1 and K_2 components of the tide. Atmospheric forcing including surface heating, net surface precipitation, surface winds and atmospheric pressure gradients for 2010-2013 came from the National Center for Atmospheric Research (NCEP/NCAR) data set. Discharges from 766 rivers are considered by the model. Discharges from US and Canadian rivers were specified by taking the daily averages of flow reports from the US Geological Survey and the Water Survey of Canada. All other river discharges were characterized by climatologically averaged daily records. AO-FVCOM also considers surface ice through a coupling with UG-CICE, the unstructured grid, finite volume version of the Los Alamos Community Ice Code developed by Gao et al. (2011).

To improve the realism of the global FVCOM, data assimilation was used to fit the model to observations. Satellite derived sea surface heights from the Aviso+ database of Le Centre National D'Études Spatiales (CNES) (http://www.aviso.oceanobs.com/en/data /products/sea-surface-height-products/global/msla.html) were assimilated south of 70°N. Satellite derived sea surface temperatures from the National Oceanographic Data Center (NODC) (ftp://data.nodc.noaa.gov/pub/data.nodc/ghrsst/L4/GLOB/NCDC/AVHRR_OI/) were also asimilated south of 70°N. This was accomplished through the mixed layer depth predicted by a Price, Weller, Pinkel (PWP) mixed layer model as described by Kantha and Clayson (1994). Finally, available temperature and salinity profiles from the NODC, Argo program, and Japan Agency for Marine-Earth Science and Technology (JAMSTEC) were assimilated into the global FVCOM on a monthly averaged basis in order to make sure that the stratification predicted by FVCOM would be consistent with observation. Following data assimilation a Mellor and Yamada (1982) level 2.5 closure scheme for vertical mixing was used in concert with a Smagorinsky (1964) closure scheme for horizontal mixing.

Here we note key trends and features of the output for selected months in each year (2012 and 2013) that will be used in the experiments. Although we will discuss depth averaged currents, significant vertical shear can lead to grossly different surface, bottom and midwater flow fields, even in the shallow Chukchi Sea. Also, there is significant realistic daily variability that at times manifests itself as a complete reversal of the the monthly mean direction. The general monthly averaged flow pattern remains remarkably stable from March to December in the Chukchi, although flow in the summer is markedly more energetic than in the winter. We choose to show July currents because this is a period when all particles in the source experiment were in motion, and September currents because this is the first month when all particles in the sink experiment

were in motion. There are several key features of each of the the flow fields that play important roles in transporting copepods to and from Hanna Shoal.

In June 2012, the Anadyr Current flow to the west of St. Lawrence Island is always more energetic than the Alaskan Coastal Current flow to the East of the Island (Figure 3-3). North of Bering Strait, the strongest flow travels to Herald Canyon. A secondary flow travels through Central Channel halfway between Herald Canyon and Hanna Shoal. After passing through the canyons, a broad, fairly strong curent follows the bathymetry to Hanna Shoal where it turns to the south before being entrained into the Barrow Canyon outflow. The modeled flow field from July 2013 (Figure 3-4) is remarakably similar to the corresponding flow from 2012. All key features mentioned above are present here. The Anadyr Current and flow through the Bering Strait are even more energetic. The only other significant difference is weakness of the Siberian Coastal Current along the southwest edge of the Chukchi, which is likely linked to the increase in flow through Bering Strait.

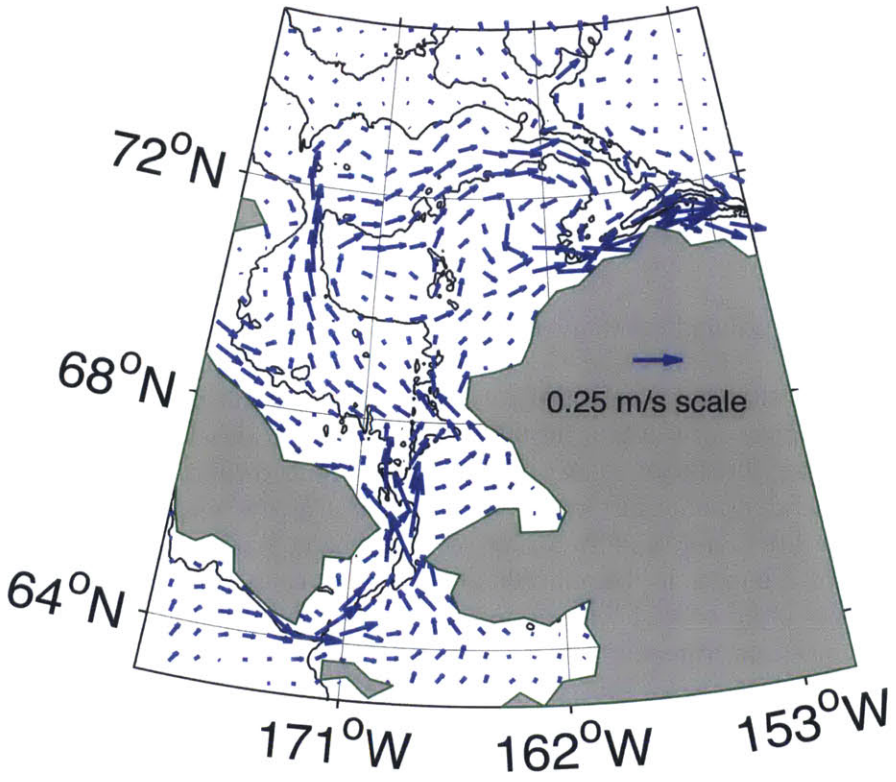

Figure 3-3: Spatially interpolated depth averaged mean modeled currents July 2012.

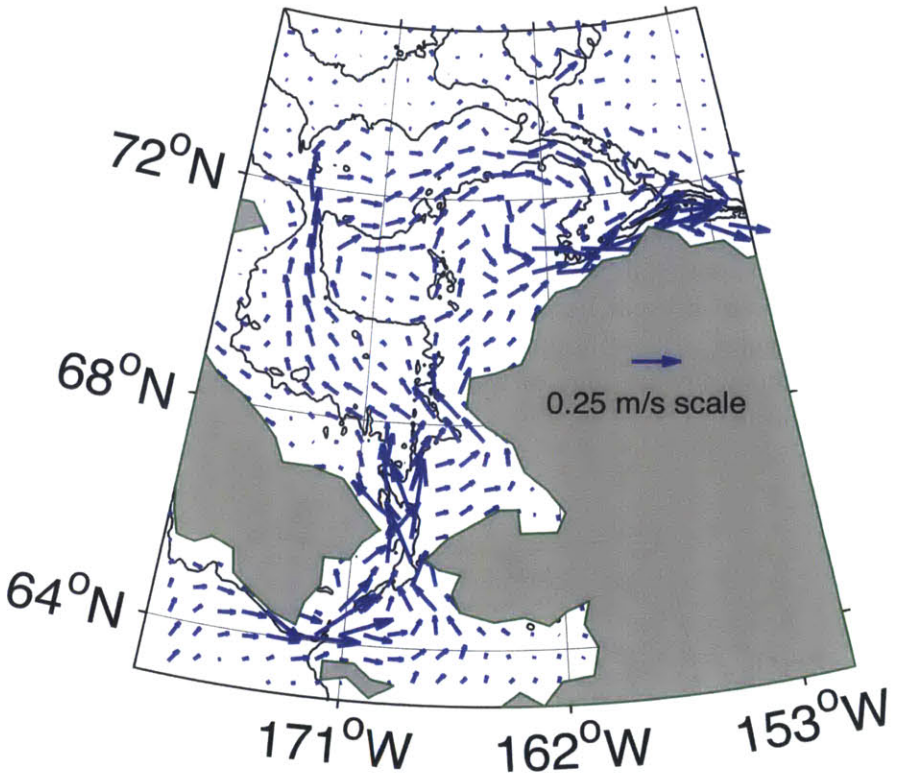

Figure 3-4: Spatially interpolated depth averaged mean modeled currents July 2013.

In September 2012, the strength of the Barrow Canyon outflow is masked by the scale of the spatial interpolation (Figure 3-5). On a monthly averaged basis this flow is strongly northward and consistent. The shellfbreak jet to the south of the Beaufort Gyre is clearly a domininent feature. The westbound countercurrent traveling from Barrow Canyon to the base of the Chukchi Cap between the southwestern corner of the Canada Basin and the northern extent of the flow from Herald Canyon to Hanna Shoal is barely visible in this presentation. That emphasizes the narrow scale of this feature and might lead us to conlcude that it would not be important in the downstream transport of copepods. As with the July flow fields, the September 2013 flow field (Figure 3-6) shares most of its characteristics with the corresponding flow field from 2012. Only two interannual differences are worthy of mention. The shelfbreak current is slightly less eneregetic in 2013. Also, the westward flowing countercurrent to the west of Barrow Canyon has a larger northward component than in 2012, but again it is almost inperceptible at this interpolation scale.

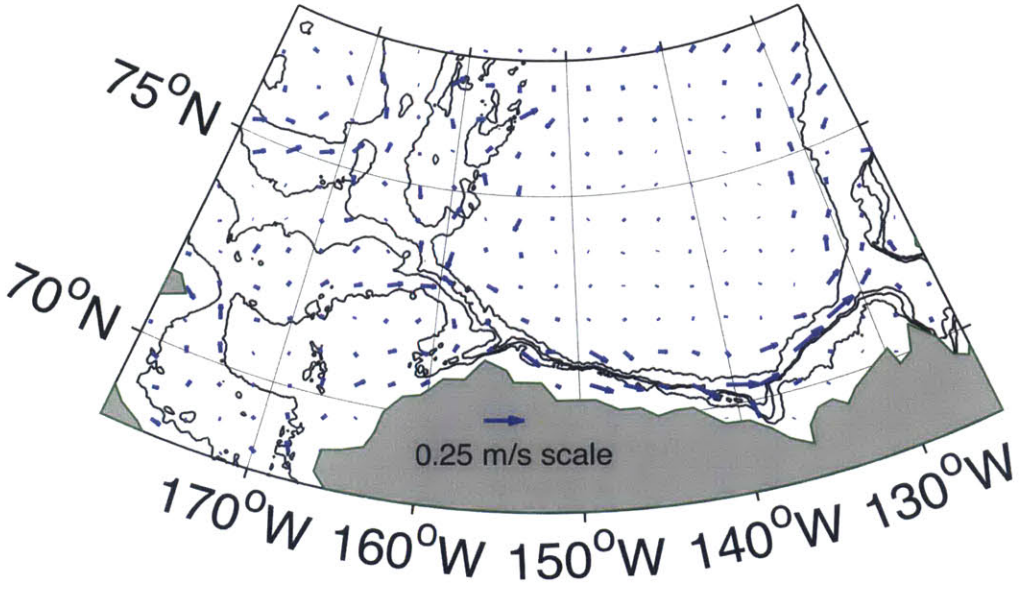

Figure 3-5: Spatially interpolated depth averaged mean modeled currents September 2012.

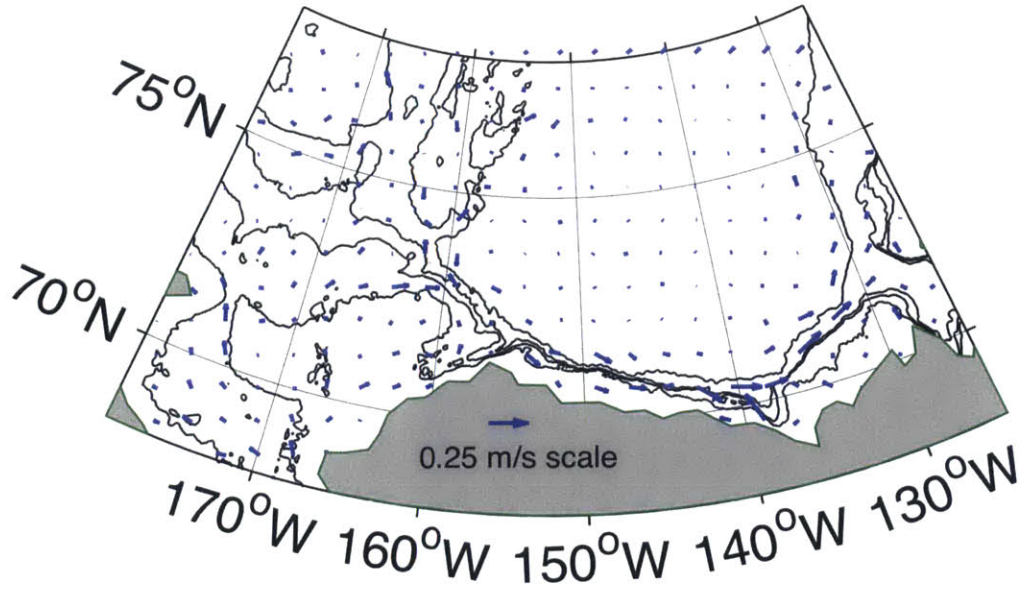

Figure 3-6 Spatially interpolated depth averaged mean modeled currents September 2013.

3.2 FISCM Configuration

A total of 46 experiments were conducted including four primary experiments based on observed distributions of *C. glacialis* and a series of 42 perturbations of the time and location of release (Table 3.2). Most parameters remained constant throughout all 46 experiments (Table (3.3); the only differences were between the 23 forward/sink and 23 backward/source experiments. All other differences between experiments were constrained to seeding and forcing.

Table 3.2: Model experiments conducted.

Number	Seeding Distribution	Class	Direction
1	2012	Primary	Forward/Sink
2	2013	Primary	Forward/Sink
3	2012	Primary	Backward/Source
4	2013	Primary	Backward/Source
5-16	2012	Spatial Perturbation	Forward/Sink
17-28	2012	Temporal Perturbation	Forward/Sink
29-31	2013	Spatial Perturbation	Forward/Sink
32-34	2013	Temporal Perturbation	Forward/Sink
35-37	2012	Spatial Perturbation	Backward/Source
38-40	2012	Temporal Perturbation	Backward/Source
41-43	2013	Spatial Perturbation	Backward/Source
44-46	2013	Temporal Perturbation	Backward/Source

Table 3.3: FISCM Parameters that remained constant across all experiments.

Parameter	Value	Meaning
mjd_offset	55775	This set the start date of the model as August, 1 2011; the first day of forcing. FVCOM works in days since November, 17 1858.
ireport	1	A single output netcdf is produced.
ngroups	1	All copepods are considered to be a single group.
year_cycle	0	None of the model runs start and end on different years.
north_pole	F	No copepods approach the North Pole.
spherical	1	The model operated in latitude and longitude.
sz_cor	0	Depths were provided instead of sigma coordinates.
fix_dep	1	All copepods stay at their depth of release.
dvm_bio	1	The copepods do not conduct diurnal vertical migration
wind_type	0	Surface winds have no direct impact on the copepods
bio_fd	0	Food conditions will not be used to control development
n_exfile	0	No forcing aside from the FVCOM output will be used.
bcond_type	1	This is a nonabsorbent boundary condition.
space_dim	3	This is a 3D experiment.
hdiff_type	0	No horizontal diffusion was used.
vdiff_type	0	No vertical diffusion was used.
biology	T	The particles will be treated as copepods with controllable times of release.
intvl_bio	30	Every five hours the development-temperature function will be run for each copepod.
start_out	0	The model will start producing output immediately.
intvl_out	144	This will publish the position and stage of all copepods once a day in a netcdf file.
BEL_ALPHA	13.04	Species specific development-temperature function parameter for C. glacialis.
BEL_A	See Below	Stage specific development-temperature function parameters for C. glacialis.

The development rate of copepods of the species *Calanus finmarchicus*, a congener of *C. glacialis*, at any specific developmental stage has been experimentally found by Campbell et al. (2001) to follow

$$D=a(T+\alpha)^{\beta} \qquad (3.2.1)$$

Where T is temperature in degrees Celsius and a, α and β are parameters fitted to experimental data. β is considered similar for all copepods. Corkett et al. (1986) found the mean β of 11 copepod species to be 2.05, so that is what we will use in this set of experiments. α is considered species specific; for *C. glacialis* we use 13.04, as determined by Corkett et al. (1986) in the lab. a is both species and stage specific. The stage specific a values for *C. glacialis* used in this

experiment were: Egg-839 N1-548 N2-819 N3-1958 N4-1070 N5-1011 N6-1186 C1-1363 C2-1905 C3-2014 C4-3057 C5-5761 (Campbell et al., 2001; Ji et al., 2012).

3.2.1 Time Step Determination

For this experiment we used a physical time step of ten minutes. This decision was reached only after careful analysis of a range of time steps from two minutes to one hour and considering the impact on accuracy and computational cost. This analysis consisted of a series of five 30 day runs using 40 particles spread across Hanna Shoal all subjected to the exact same forcing and model parameters. The test distribution considered 20 particles spread across the shoal at 1 meter depth and 20 particles spread across the shoal at 40 meters depth. All 40 particles were released at the same time on August 1st 2013. The model was run on a single core of a Intel E5-2680 v2 CPU running at 2.80GHz as part of Woods Hole Oceanographic Institution's (WHOI) scientific computing cluster.

For the purpose of this exercise the 2 minute time step was treated as the best representative of true advection and all other time steps were compared to it. At the end of each day, the position of each particle in each experiment was compared to the position of the corresponding particle in the 2 minute time step run. The 40 distances for each of the particle pairs were summed to make a single value for each day (Figure 3-7).

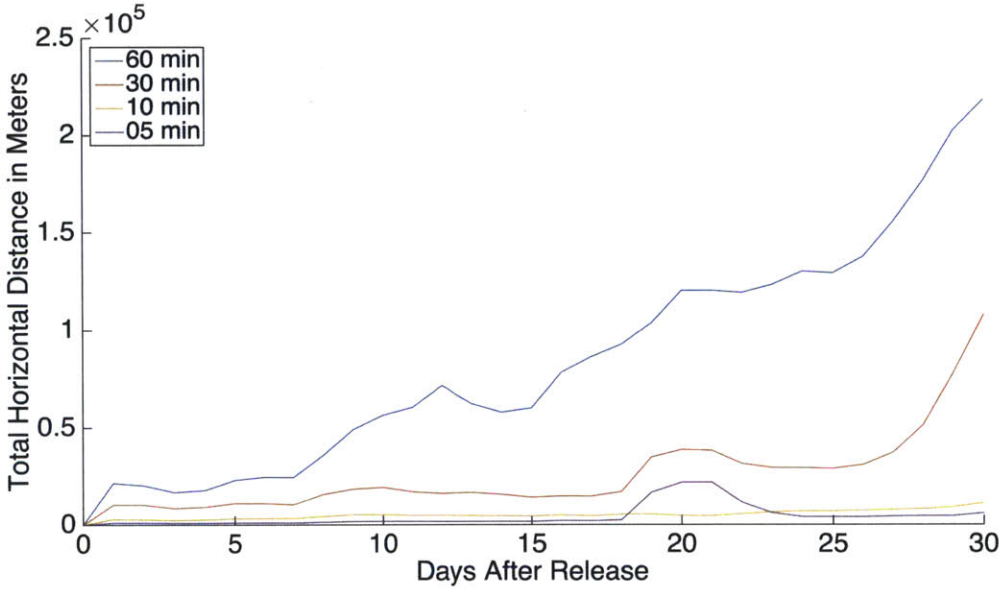

Figure 3-7: The total horizontal distance between 40 particles released over Hanna Shoal and their corresponding particles released in a 2 minute time step model run.

At the end of the first day of the run the particles diverge, but aside from one point around day 20 the smaller time step runs always stay closer to the 2 minute run than the larger time step runs. This event around day 20 was found to be linked to the time that particles were leaving Hanna Shoal via Barrow Canyon. Since the currents are much faster in the canyon, precise timing of a particle arriving in the middle of this flow could lead to significant horizontal differences.

If we only consider the positions of the particles at the end of day thirty and we convert the total horizontal difference to a sum of squared errors we can evaluate how this quantity is affected by the time step of a given run (Figure 3-8). We obtained empirical results that appear to be close to third order convergence by examining the rate with which the error is reduced as we refine our time grid.

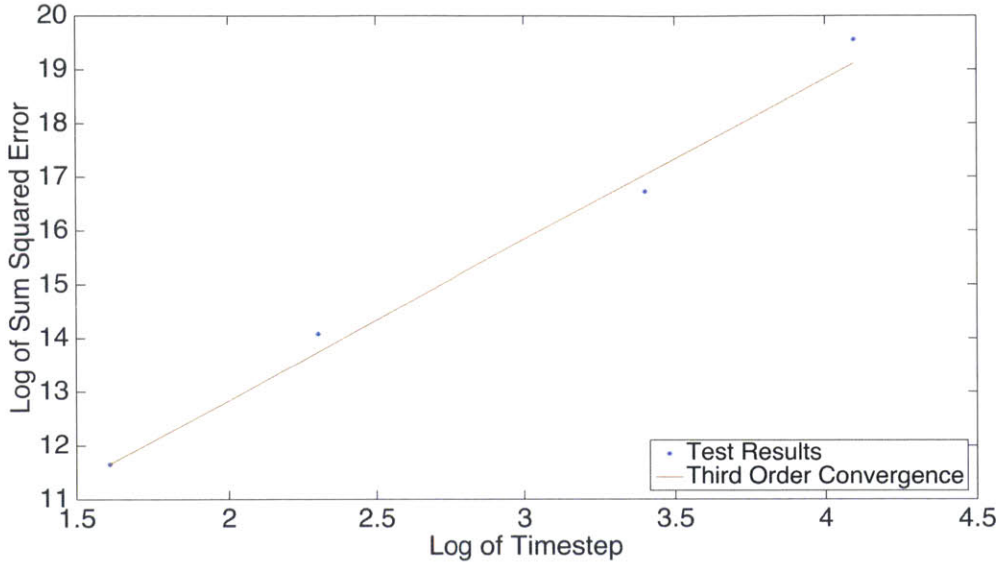

Figure 3-8: Sum squared error at day 30 of the time step test for different time steps compared to a run with a two-minute time step. Each refinement of the time grid results in an approximately third order reduction in error.

These runs took between 62 and two minutes to execute for the two and 60 minute time step tests respectively. Plotted on a log scale against the log of the corresponding time step (Figure 3-9) we see that the decrease in computational time with increasing time step follows a first order relationship.

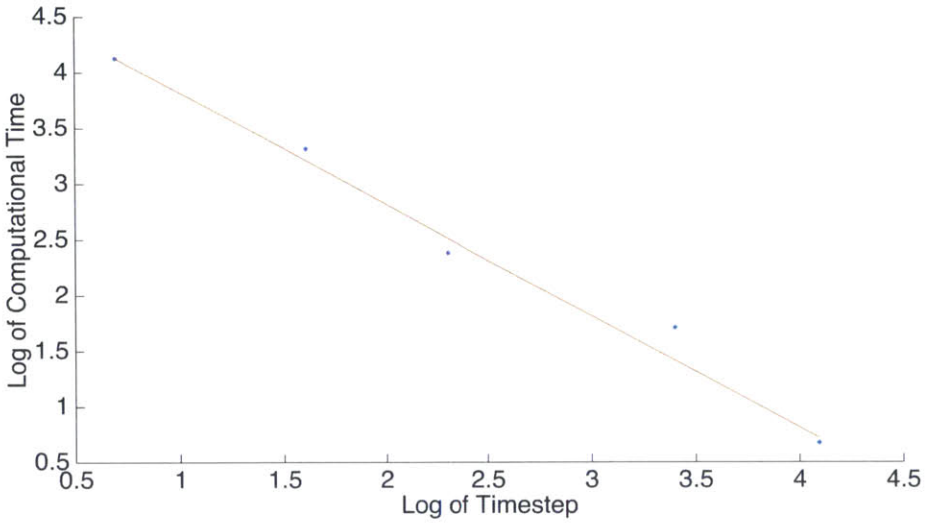

Figure 3-9: Computational time for the 30 day run using different time steps. Each coarsening of the time grid results in a first order reduction in computational time.

The 10 minute time step emerges from this analysis as the clear choice. It both maintains a relatively small error compared to the 2 minute run and carries a computational cost six times less than the 2 minute run and 3 times less than the 5 minute run. Working again with a single core of an Intel E5-2680 v2 CPU running at 2.80GHz as part of WHOI's scientific computing cluster, the full experiments discussed throughout this work took approximately six hours to run.

3.2.2 Sink and Source Experiments

The sink experiments were designed to identify the regions in the Western Arctic that were supplied with copepods originating on Hanna Shoal. These experiments were run for the time period of August 1st through December 15th for both 2012 and 2013 (Table 3.4) using FVCOM forcing for the last five months of the year in question. The 15th of December was chosen as a representative date when all surviving *C. glacialis* individuals enter diapause if they have developed sufficiently. Throughout these experiments the juvenile copepods developed according to (Equation 3.2.1) based on the temperature they experienced. Mortality was not considered. The distributions of diapause capable (copopodid 4 and above) copepods from Hanna Shoal on the final day were compared interannually and the sensitivity of these solutions were tested through the perturbation analyses.

Table 3.4: FISCM Parameters that varied between source and sink experiments.

Parameter	Sink Value	Source Value	Meaning
beg_time_days	366 or 731	396 or 761	The model day the experiment started in 2012 or 2013.
end_time_days	502 or 867	215 or 580	The model day the experiment ended in 2012 or 2013.
deltaT	600	-600	This is the physical time step in seconds
nfiles_in	5	7	This is the number of FVCOM forcing files used
Tnind	950574	950578	The total number of copepod in the experiment.

The source experiments were designed to identify the regions that were supplying copepods to Hanna Shoal. These experiments were run for the period of August 31st backwards to March 3rd for both 2012 and 2013 (Table 3.4) using FVCOM forcing for September backwards through March of the year in question. The 3rd of March was chosen as a representative date when *C. glacialis* adults in the Bering Sea and southern Chukchi begin being active. Throughout these experiments juvenile copepods observed over Hanna Shoal undergo neoteny, or juvenilization as they iterate backward through developmental stages according to (Equation 3.2.1) based on the temperature they experience. When a copepod descends below the egg stage, it is stopped, as this is the putative location where it was released from its parent. Since the ages of the adult copepods collected on Hanna Shoal were not known, we choose to have adults remain adult for the duration of the experiment. This simulates that the adults we observed over Hanna Shoal matured to at least copopodite 4 during the previous growth season.

To allow for this, a new status was added to FISCM: 'HATCHED'. A better name would have been 'RELEASED' as it is really when the eggs are released by the female and not when the eggs transition to nauplii 1. This new status accomplishes three things; it better approximates the current understanding of the *C. glacialis* life cycle in the western Arctic, it avoids an error that occurs if FISCM tries to juvenilize a copepod whose stage is less than 1 and it removes them from the active pool of particles, significantly speeding up the remaining calculations. After only two months only the adults remain active in the experiment.

It is important to recognize that FISCM does not attempt to simulate predation or mortality. This means in the forward/sink configuration FISCM is showing areas that have the physical potential to hold mature copepods later in the year. If the distribution experiences uneven mortality and predation the shape of the resulting distribution could be dramatically different. In the backward/source configuration, FISCM is showing the regions that supplied copepods to Hanna Shoal. In no way is it attempting to recreate the population of copepods earlier in the year, as such a population suffered mortality and predation as it moved to Hanna Shoal. For each successful arrival, there were likely many more that left the source region. What FISCM does show us is maximum possible spatial extent of the sink region and the minimum possible extent of the source region.

3.3 Seeding Configuration

Seeding for the primary experiments was driven by observed distributions. In August 2012 and 2013, USCGC HEALY conducted two cruises in the Northeast Chukchi Sea in support of the Hanna Shoal Ecosystem Study, an extension of the Chukchi Sea Offshore Monitoring in Drilling Area study. Both projects are multi-disciplinary investigations funded by BOEM to examine the biological, chemical and physical properties that define the Hanna Shoal ecosystem. Our participation was focused on the distributions of zooplankton. Between 13 and 23 August in 2012 and 1 and 14 August in 2013, vertically integrated tows were conducted at different sites across the geographic extent with particular attention given to areas around the periphery (Figure 3-10). The exact choice of the 34 sites sampled in 2013 was driven by a desire to both reoccupy some sites among the 26 sampled in 2012 and expand the overall spatial extent of the dataset.

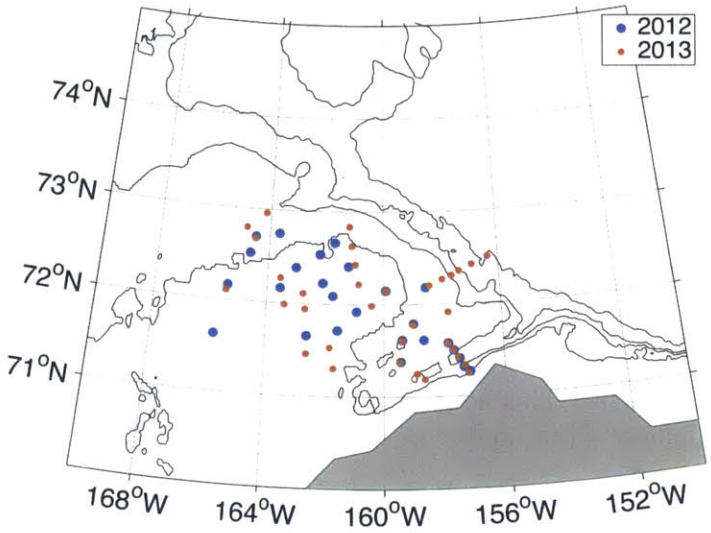

Figure 3-10: Sites sampled over Hanna Shoal in August of 2012 and 2013.

At each site, paired 50 cm diameter Bongo nets equipped with 150 μm and 500 μm mesh were towed vertically from 5 m off the bottom to the surface. The contents of the 150 um net were carefully transferred into plastic jars. Buffered formalin was added for transport back to the lab. Samples were sent to C. Gelfman at the University of Rhode Island for identification to species level where possible. *C. glacialis*, *C. hyperboreus* and *Pseudocalanus spp.* individuals were identified to life stage. *C. glacialis* nauplii and eggs are too small to be sampled quantitatively using a 150 μm net, so although they were observed and counted they were not used in the analyses or model experiments.

The *C. glacialis* counts in the samples were scaled to number of individuals at each life stage per square meter. If we represent each station with by one square meter of sea surface, this results a total of 950,574 individual *C glacialis* stages copopodid one through adult observed in 2012 (Figure 3-11) and 803,532 in 2013 (Figure 3-12). It should be noted that no adult males were observed in 2012. Both years show a clear skew in numbers towards earlier stages as would be expected based on when the samples were taken relative to the *C. glacialis* growth season. This skew is more intense in 2012 when observations of adults were only made at 50% of the stations. Also during both years, later stages are found in higher numbers in Barrow Canyon and on the eastern extremis of the shoal, while earlier stages were more common over the center and western extremis of the shoal. The notable exception to this pattern is the distribution of copepodid fours in 2013, which has a strong peak at the furthest west site sampled.

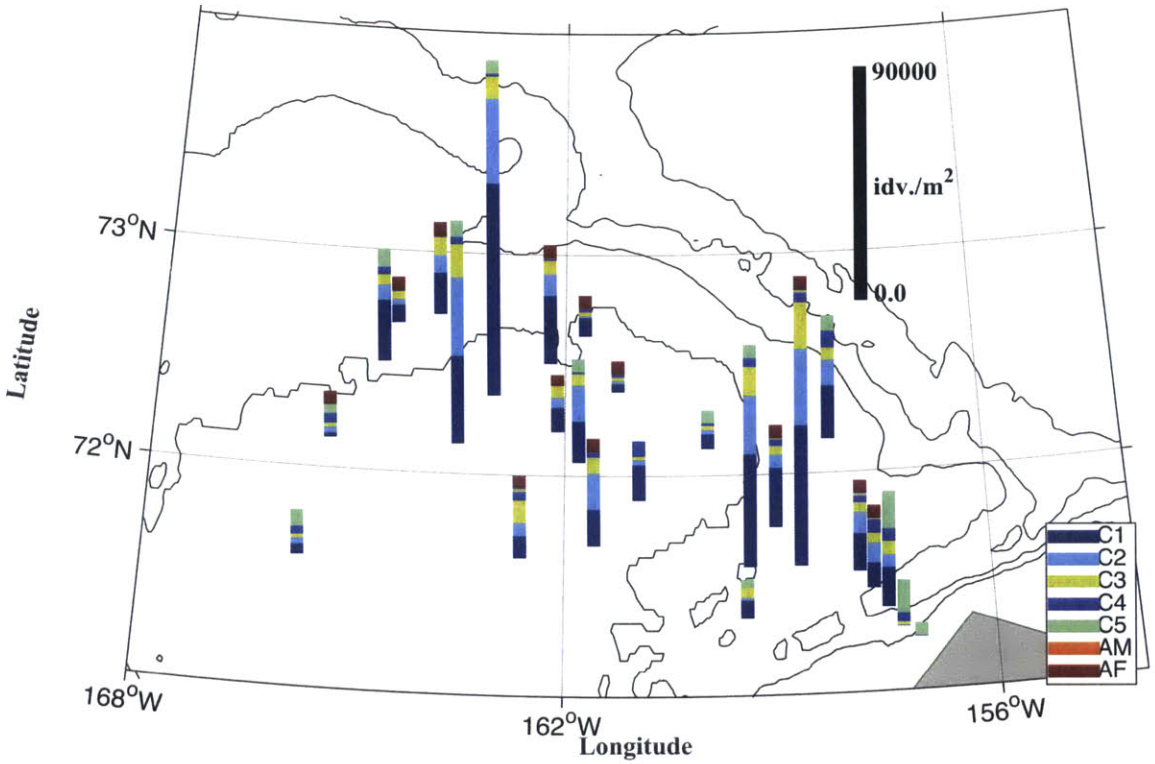

Figure 3-11: Observed density (idv/m^2) of *C. glacialis* over Hanna Shoal in 2012.

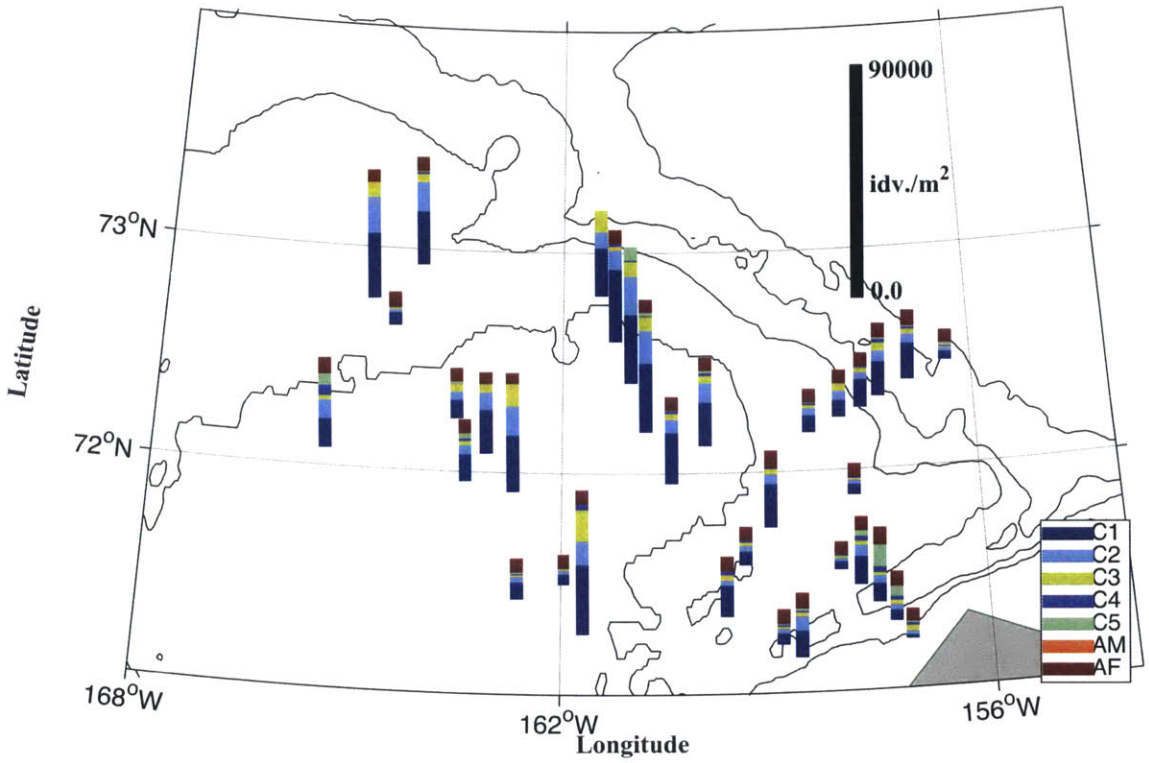

Figure 3-12: Observed density (idv/m^2) of *C. glacialis* over Hanna Shoal in 2013.

Fewer copepods were observed in 2013 despite sampling eight more sites (Figure 3-12). In general the distribution is much more even, but there does seem to be a general pattern of greater abundances in the west. Copepodid stage one remains by far the most represented life stage, but the relative contribution from adult females is much larger. There are relatively fewer copepodid stage fives and they are less dominant in eastern Barrow Canyon despite still being present.

We use these observed distributions to drive our seeding instead of the more classic IBM approach of using a uniform distribution across the spatial domain of interest. The primary experiments (Table 3.2.1) used either seeding based on the 2012 or 2013 observed distribution. At each sampling site we seed the water column with the full number of *C. glacialis* at each stage observed at the time of the sampling. In order to make results from the two years entirely comparable, the observed distribution in 2013 was scaled up by 1.183 to result in the almost the same total number of particles ($950574 \approx 950578$). This had no effect to the relative contribution from different stages or different sampling locations. Since the numbers were acquired through vertical net tows, it is not possible to know the vertical distribution pattern. For this reason, the model copepods are spread evenly between the 45 depth layers represented by FVCOM. The remainder was placed in the surface layer. All sampling sites had depths less than 225 m, so the layers were always evenly spaced. The perturbation experiments (Table 3.2.1) used modifications of these two primary seeding distributions that will be described below.

The most up to date version of FISCM lacked the ability to set the starting stage for a copepod being released. Released copepods always started as eggs. Not only would this prevent us from representing our observed distribution for the forward run, it would make running the model in reverse impossible. By modifying the gparms.f90 and modbio.f90 files we were able to introduce a new variable "initstage". This modification simply requires the user to include a sixth column in the initialization file corresponding to the stage of the copepod at time of release.

3.4 Perturbation Analysis

Clearly the *C. glacialis* distribution over Hanna Shoal is much more continuous than 26 observations made across two weeks and the currents over the shoal are highly variable, particularly in Barrow Canyon. The result of tracking the source or sink of these specific copepods alone would never allow us to draw meaningful conclusions regarding patterns of physical control over the entire shoal. They could lead us to overly inflate the importance of source and sink regions that in reality are only important to the 26 point/time combinations sampled. Our conclusions would be strongly biased by the very arbitrary exact times and locations of our sampling effort.

One approach to resolving this discrepancy would be to interpolate our observations across space and start with a more continuous seeding distribution, however the temporal difference between observations could lead us to conflate spatial and temporal variability. Since we do not have multiple observations at the same station during the same year we also have no way of interpolating solely in time. In addition, representing a distribution of copepods as a smooth interpolation would ignore the inherent patchiness of the real distribution. Given this reality we opted to take the approach of perturbation analysis.

Each observed distribution was perturbed both in time and space. For the 2012 forward/sink experiment, 12 of each perturbation were completed. For the other three primary experiments,

only three of each perturbation were completed (Table 3.2). Perturbations were achieved using the "rand" function in MATLAB, which outputs a number between zero and one from a uniform distribution of pseudorandom numbers. In temporal perturbations each of the observation times were modified by up to 40 hours in either direction using a call to "rand" for the sign of the change and a call to "rand" for magnitude of the change. In spatial perturbations each of the observation positions was modified by up to 14.14 km using four calls to "rand". The horizontal coordinate was modified by up to 10 km in either direction and the vertical coordinate was modified by up to 10 km in either direction. The scale of the spatial perturbation was chosen to correspond roughly to the horizontal resolution of the model, meaning it could move the release point to one of the three neighboring control volumes. The scale of the temporal perturbation was chosen to correspond roughly to the possibility of moving the release time up to 1.5 days earlier or 1.5 days later.

By comparing the results of individual perturbation experiments and the corresponding primary experiment we were able to see the sensitivity of the "solution" to small-scale (in terms of the model resolution) temporal and spatial changes in the physical forcing. By looking at a perturbation mean and comparing it to the results of the primary experiment, we could find regions that were not found to be important in the primary experiment, but have the physical potential to be important. The differences we observed between the results of 2012 and 2013 primary experiments could be the result of interannual differences in the biological conditions, differences in the physical forcing, or the semi-arbitrary times and locations of sampling. The differences between the 2012 and 2013 perturbation means were by and large the result of interannual differences in physical forcing.

3.5 Statistical Methods

The end product of a FISCM experiment is a list of the position and developmental stage of the copepods released. We convert this to a probability distribution by creating a two dimensional histogram with a 5 km grid spacing and then dividing by the total number of copepods in the experiment. Because horizontal diffusion was disabled, very few grid cells across the domain actually contain copepods and those that do have very large numbers of them. Because this implies a level of determination that we do not have, we pass a Gaussian filter over the probability distribution twice. The filter is passed in the x direction first and then in the y direction. The filter is the length or width of the domain as appropriate and has a standard deviation of 12.5 km. This procedure allows us to better represent the uncertainty inherent in our solution.

The perturbation mean distribution is created by adding together the results of the relevant experiments, then dividing by the number of experiments involved. In this way the sum of the perturbation mean distribution remains one. For the 2012 forward/sink experiment we will compare the means using 3, 6 and 12 perturbations. In the other three primary experiments we will only calculate a mean using the 3 perturbations conducted. We then proceed to use a number of methods to compare the different distributions.

We term the simplest approach "Variation". It is formed by simply subtracting one distribution from the other, taking the absolute value of each grid cell, summing across all grid cells and dividing by two (3.8.1). This approach makes no distinction between several small differences

and a single large difference. It also does not discriminate between large and small offsets.

$$V = \Sigma |P_1 - P_2|/2 \qquad (3.8.1)$$

In order to discriminate between small and large offsets and deflate small differences we first threshold the distributions by eliminating all values lower than 10^{-4} and term what remains a hotspot. Hotspot analysis works best when looking a single feature or cluster of features. In the sink experiments we created an east and west hotspot for each distribution using the exit from Barrow Canyon at 155°W as the dividing point. In the source experiments we created three hotspots, one for the egg release points and two for the adult distributions. We split each adult distribution at Bering Strait (65.8°N) to create a north and south hotspot.

The hotspots for different distributions were compared using two different methods. The first was a center of mass comparison and the second was a modification of Rose et al.'s (2009) Slip and Slide method for comparing spatial model output.

The center of mass for each hotspot was calculated by taking the result of the two dimensional histogram with a 5 km grid spacing and finding the gray-level-weighted center of mass in units of pixels. This position was then projected into the projected coordinates for either the source or sink experiment as appropriate. Comparisons were then made by taking the straight line distance in projected coordinates between two centers of mass.

To use the slip and slide method we optimize the parameters in equations (3.8.2-3.8.3) that minimize the differences between the hotspots generated by two different model runs using the MATLAB function "fminsearch".

$$x_{new} = (y \times \sin(\theta_r) + x \times \cos(\theta_r)) \times M_x + A_x \qquad (3.8.2)$$

$$y_{new} = (y \times \cos(\theta_r) - x \times \sin(\theta_r)) \times M_y + A_y \qquad (3.8.3)$$

Where x and y are the coordinates of all copepod location probabilities in a two dimensional matrix. θ_r is the rotation applied to the hotspot being manipulated. M_x and M_y is the degree to which the hotspot being manipulated is stretched or squeezed in each direction. A_x and A_y is the degree to which the hotspot being manipulated is slid in each direction. x_{new} and y_{new} are the new coordinates of the manipulated hotspot.

"fminsearch" uses multidimensional unconstrained nonlinear minimization, specifically the Nelder-Mead simplex direct search method to find the parameters in equations (3.8.2-3.8.3) that minimize a residual function, in this case defined as the percent variation (3.8.4) between the two model hotspots.

$$PV = \Sigma |P_1 - P_2|/\Sigma (P_1 + P_2) \qquad (3.8.4)$$

Where PV is percent variation, P_1 is the two dimensional matrix of copepod location probabilities in the hotspot that will be manipulated and P_2 is the two dimensional matrix of copepod location probabilities in the hotspot that will be used as reference, typically a perturbation mean or a different year in the case of interannual comparison.

The hotspots start off on the exact same grid, but after manipulation one grid is no longer uniform. A gridded linear interpolant is defined to permit the residual function to query the manipulated hotspot at all the points for which it has values in the reference hotspot. The application of this method not only allows us to better quantify the difference between two model outputs, it also allows us to better characterize the differences themselves.

Chapter 4

Results

4.1 Sink Experiment 2012

This simulation tracked the locations to where *C. glacialis* observed on Hanna Shoal in August 2012 were advected by December 2012. The 2012 sink model run suggests that the vast majority of the copepods over Hanna Shoal enter diapause over the shelfbreak at the southern extent of the Canada Basin and along the southeastern buttress of the Chukchi Cap (Figure 4-1). A significant concentration also occurs along the coast to the east of Barrow. On December 15th only a very small number remain over Hanna Shoal. Those on the northern tip of the shoal were typically first advected around the shoal before being ejected through Barrow canyon and traveling west.

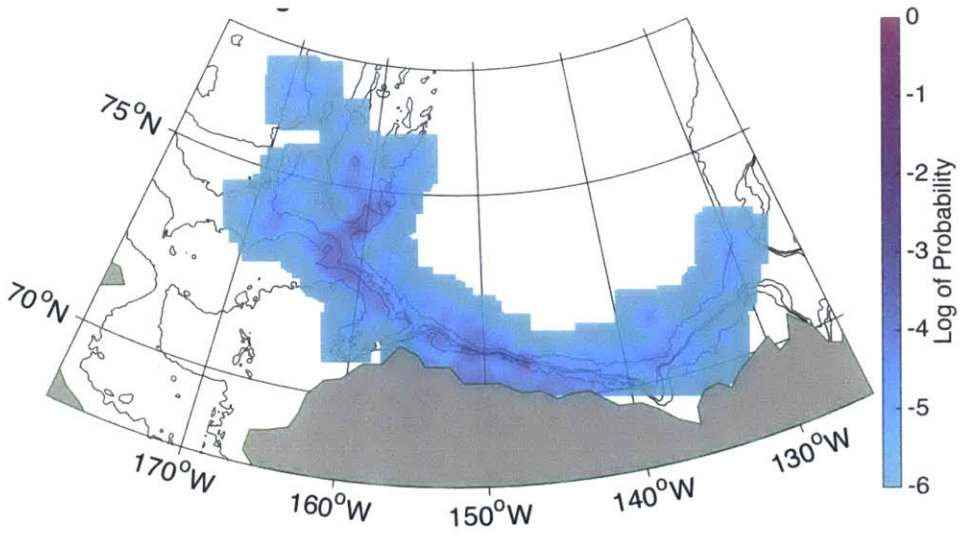

Figure 4-1: Filtered Probability Distribution Of Adult *C. glacialis* on 15 December 2012.

Once all probabilities below 10^{-4} are eliminated to create the hotspots we see that the eastern and western extremes of the distribution are not as important as they first appeared (Figure 4-2). The two key sink regions are a western area at the southeastern buttress of the Chukchi Cap and an eastern area split between the coast and the shelfbreak halfway from Barrow to the Canadian border.

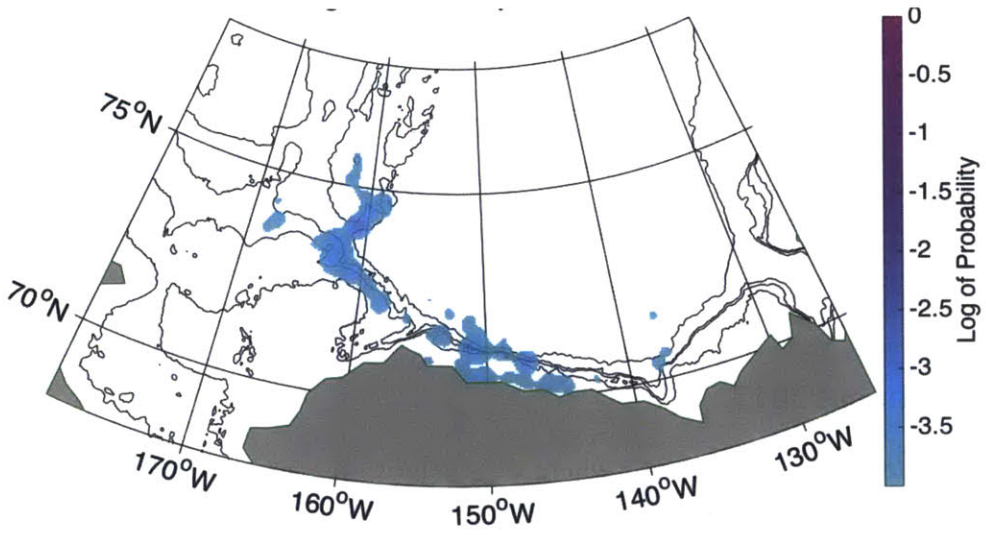

Figure 4-2: Hotspots from the Filtered Probability Distribution Of Adult *C. glacialis* on 15 December 2012.

The simplistic model used in this experiment assumes food saturation and only temperature constrains development. Although food (often in the form of microzooplankton) is in good supply in August, this would be a very poor assumption to make throughout the fall and beginning of winter. What we see however is very fast development: 50% of our copepods are competent to diapause by September 21 and 90% are competent to diapause by September 30 (Figure 4-3). Thus, critical development is complete before food conditions would become limiting. Although many of these copepods would have been consumed by predators, we believe the vast majority of the copepods we observed had the potential to survive until diapause.

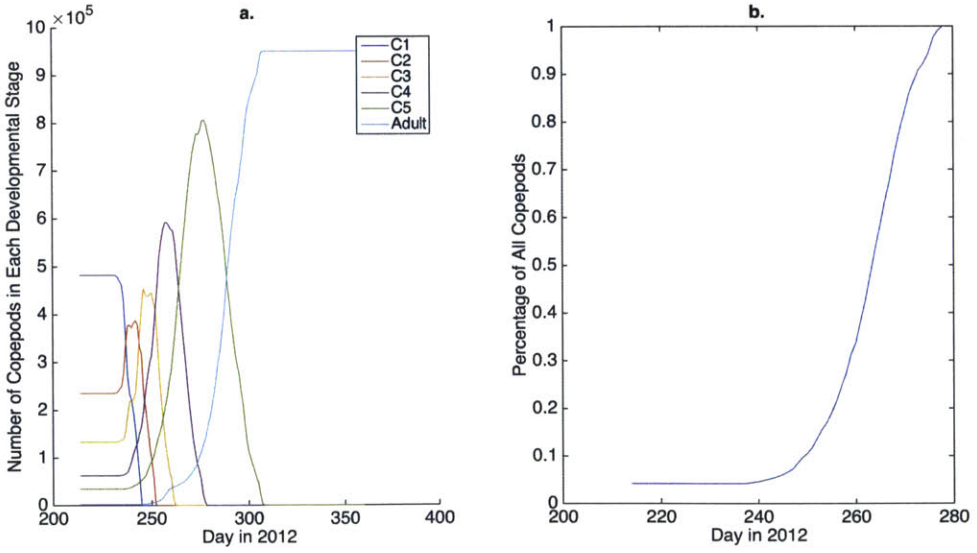

Figure 4-3: Development in 2012: a. The number of modeled copepods at each stage. b. The percentage of copepods competent to diapause (copepodid stage four or later).

4.2 Sink Experiment 2013

This simulation tracked the locations to where *C. glacialis* observed on Hanna Shoal in August 2013 were advected by December 2013 under the slightly different circulation regime observed in that year. In the 2013 sink model run, the shelfbreak and the southeastern buttress of the Chukchi Cap remain important, but the entire distribution is shifted west with many more copepods ending up on the Chukchi Cap instead of just along its periphery (Figure 4-4). Also of note is the presence of copepods across Hanna Shoal, albeit in much smaller numbers than elsewhere.

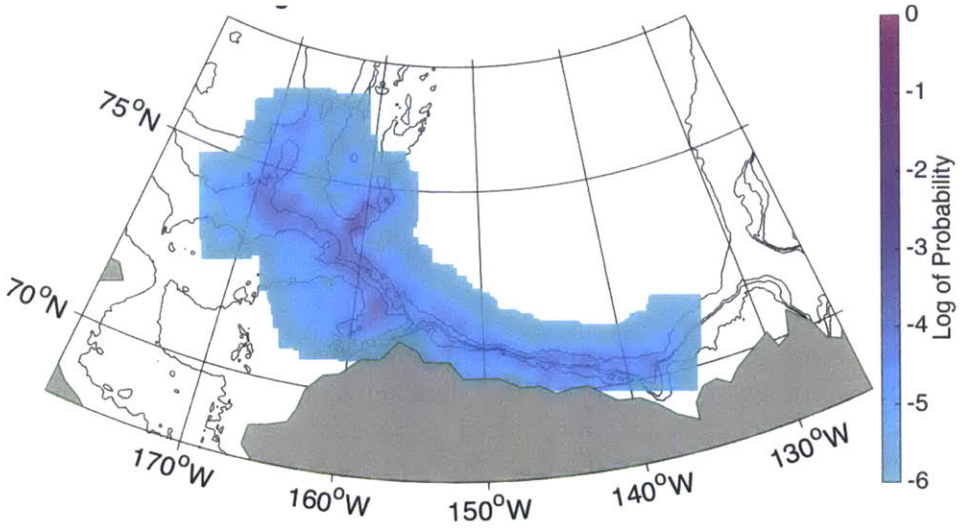

Figure 4-4: Filtered Probability Distribution Of Adult *C. glacialis* on 15 December 2013.

The western sink region is more important in 2013 than in 2012 and it extends all the way around the northern tip of Hanna Shoal. The eastern sink region is much less concentrated and is constrained to the shelfbreak, lacking the inshore concentration observed in 2012 (Figure 4-5).

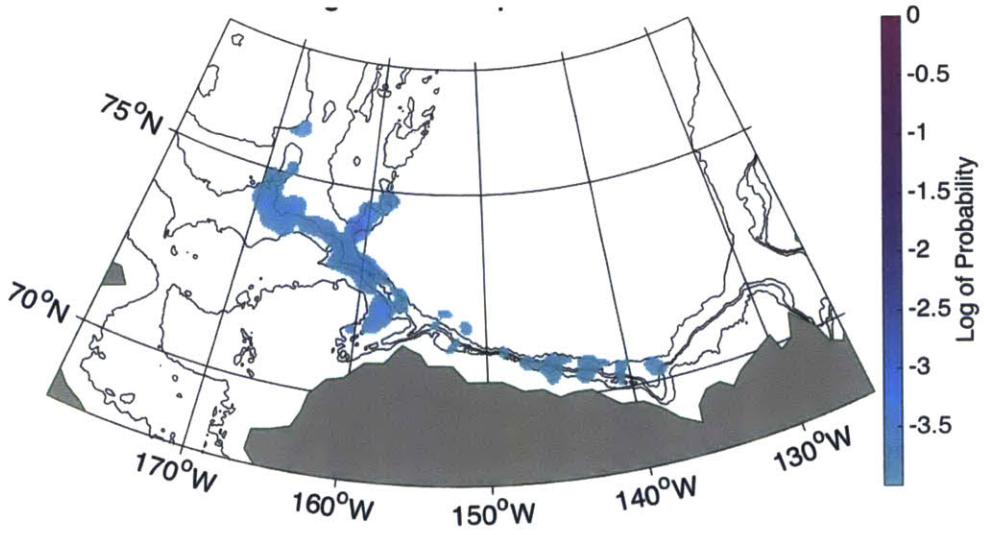

Figure 4-5: Hotspots from the Filtered Probability Distribution Of Adult *C. glacialis* on 15 December 2013.

Despite 2013 having more Arctic ice at the summer minima than 2012, water temperatures around Hanna Shoal were even warmer in 2013 leading to even faster development in our modeled copepods. Fifty percent of our model copepods are competent to diapause by September 11 and 90% are competent to diapause by September 21 (Figure 4-6). This being the case, the assumption regarding food saturation is even less problematic in 2013 than it was in 2012.

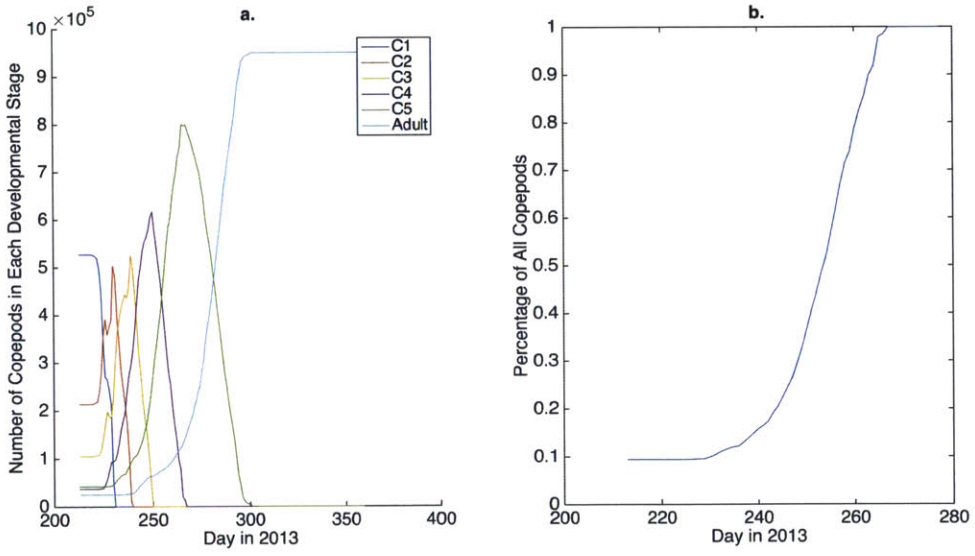

Figure 4-6: Development in 2013: a. The number of modeled copepods at each stage. b. The percentage of copepods competent to diapause (copepodid stage four or later).

4.3 Source Experiment 2012

This simulation tracked the *C. glacialis* observed on Hanna Shoal in August 2012 backward to see where they would have been in March 2012. The results suggests that the adult copepods observed over Hanna Shoal in August 2012 came from the south and west, with only a very small proportion starting over the shoal itself (Figure 4-7). The distribution almost covers the entire Chukchi, but is skewed to the west, particularly at the northern and southern extent. By May 1 all the juvenile copepods had aged back to their putative release. The egg release distribution is accordingly skewed towards the northern portion of the domain. Because this portion of the experiment effectively had less time to run, it makes sense that the distribution of egg release sites is much less dispersed than the adult starting position distribution.

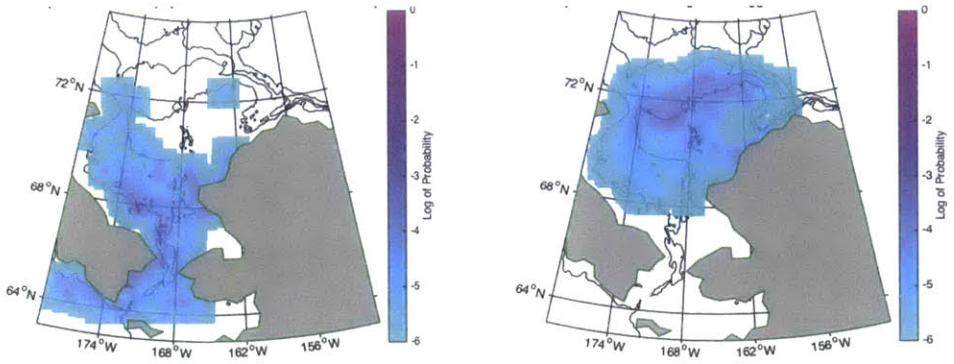

Figure 4-7: Filtered probability distributions of adult *C. glacialis* on 03 March 2012 (Left) of *C. glacialis* egg release locations (Right).

The source regions for the adults are not particularly cohesive. The weaker southern region south of the Bering Strait is strongly skewed to the west (Figure 4-8). The stronger northern region includes branches pointing toward Herald Canyon, the Central Channel and the Coast of Alaska. The source region for the juveniles is centered in the broad slope that connects Hanna Shoal with Herald Canyon, although there are a few small regions in the Central Channel and along the Alaskan coast.

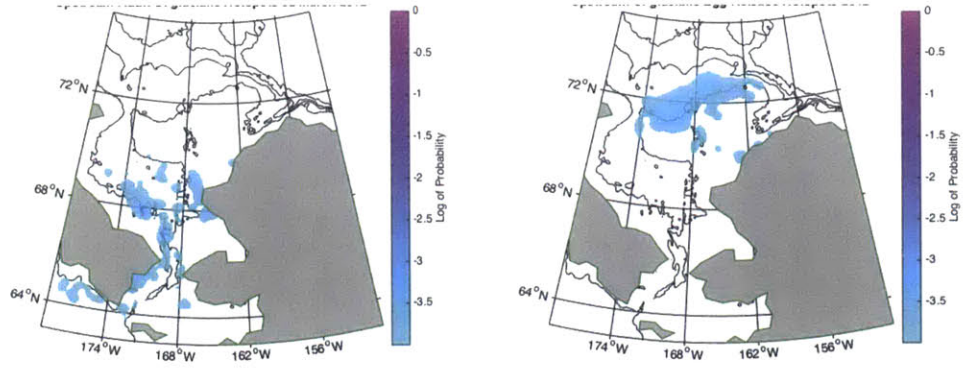

Figure 4-8: Hotspots from the filtered probability distributions of adult *C. glacialis* on 03 March 2012 (Left) and of *C. glacialis* egg release locations (Right).

4.4 Source Experiment 2013

This simulation tracked the *C. glacialis* observed on Hanna Shoal in August 2013 backward under the slightly different circulation regime observed in that year to see where they would have been in March 2013. The 2013 source experiment produced similar results to the 2012 experiment; in general it is south and west of Hanna Shoal (Figure 4-9). The biggest differences are that some of the copepods came from the Beaufort, more came from the northwest Chukchi and fewer were in the Bering on 3 March.

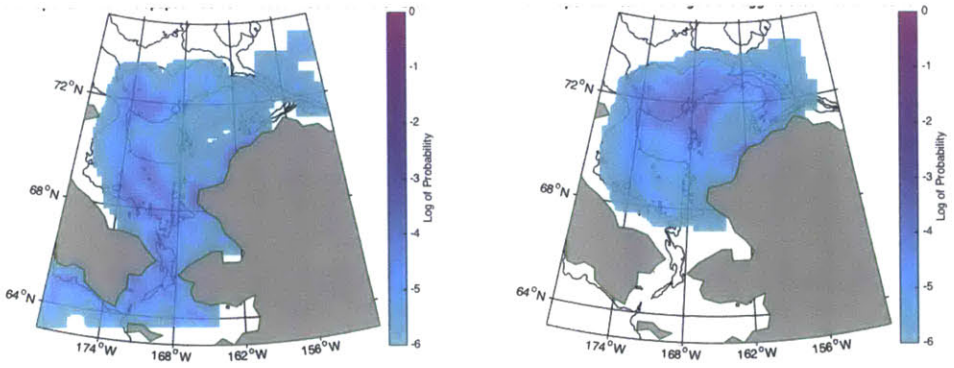

Figure 4-9: Filtered probability distributions of adult *C. glacialis* on 03 March 2013 (Left) and of *C. glacialis* egg release locations (Right).

Once hotspots are identified, the source regions south of Bering Strait are small and scattered (Figure 4-10). The source regions north of the Strait are mainly in the same three segments as seen for 2012, but there is a fourth region between the exits from Herald Canyon and Central Channel implying that many of the Hanna shoal copepods started the 2013 growth season far to north of where the 2012 stock started their growth season. The source region for juveniles is centered on the north end of the Central Channel, halfway between Herald Canyon and Hanna Shoal. There are two small secondary regions over Hanna Shoal and along the Alaskan coast.

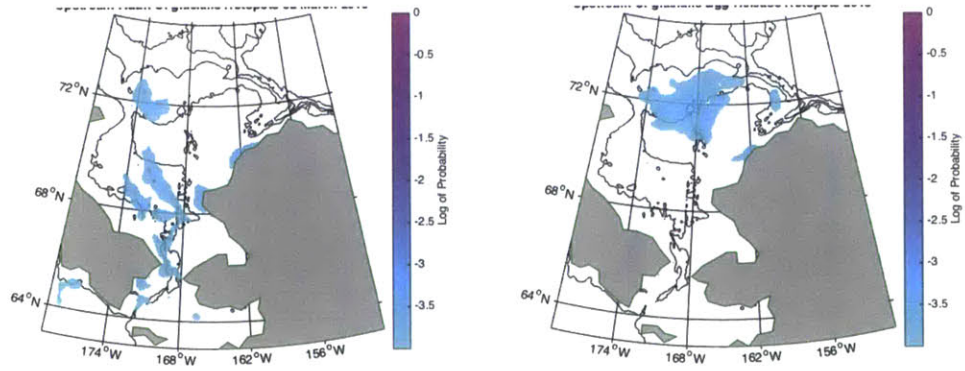

Figure 4-10: Hotspots from the filtered probability distributions of adult *C. glacialis* on 03 March 2012 (Left) and of *C. glacialis* egg release locations (Right).

4.5 Interannual Comparison

In comparing the results of the sink experiments between the two years, we find several cohesive regions where the 2013 distribution is stronger and two where the 2012 distribution was stronger (Figure 4-11). The westward shift of the distribution in 2013 is striking, particularly the large concentration traveling over the Chukchi Cap and the high concentration just to the west of Barrow Canyon. Although copepods in the 2012 experiment reached the Eastern edge of the Canada Basin their numbers were small. The number found along the northern Alaskan coast however was very sizable and entirely absent in 2013.

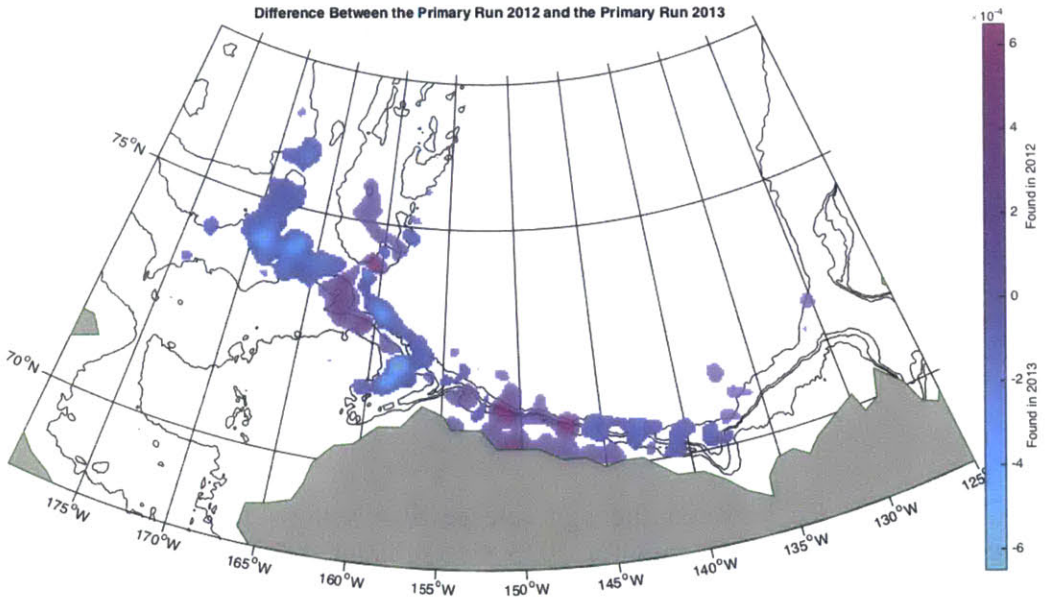

Figure 4-11: The difference between the 2012 and 2013 primary sink experiments. The result for 2013 was subtracted from the 2012 result and all values greater than $5x10^{-5}$ were retained. Purples indicate sink locations for 2012 but not 2013 while lighter blues indicate sink locations for 2013 but not for 2012.

By contrast, the differences between the 2012 and 2013 egg release distributions are highly cohesive (Figure 4-12). Harold Canyon and the shallower portion of the broad slope east of the exit from Harold Canyon are more important in 2012. The deeper portion of this slope and Hanna Shoal itself are more important in 2013.

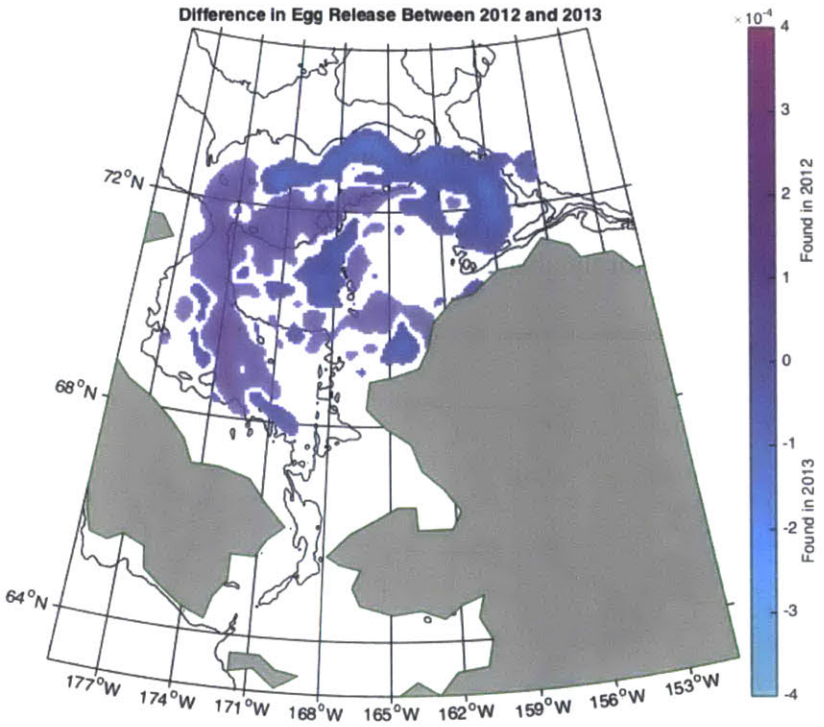

Figure 4-12: The difference between the egg release distributions from the 2012 and 2013 primary source experiments. The result for 2013 was subtracted from the 2012 result and all values greater than 5x10-5 were retained.

The differences between the 2012 and 2013 distributions of adults from the source experiments (Figure 4-13) are the least cohesive of the three interannual comparisons. This is partially due to the fact that these distributions included far fewer copepods than the others, and thus one would expect a more patchwork response. There was a southward shift in the distribution in 2012 and a northward shift in the 2013 distribution.

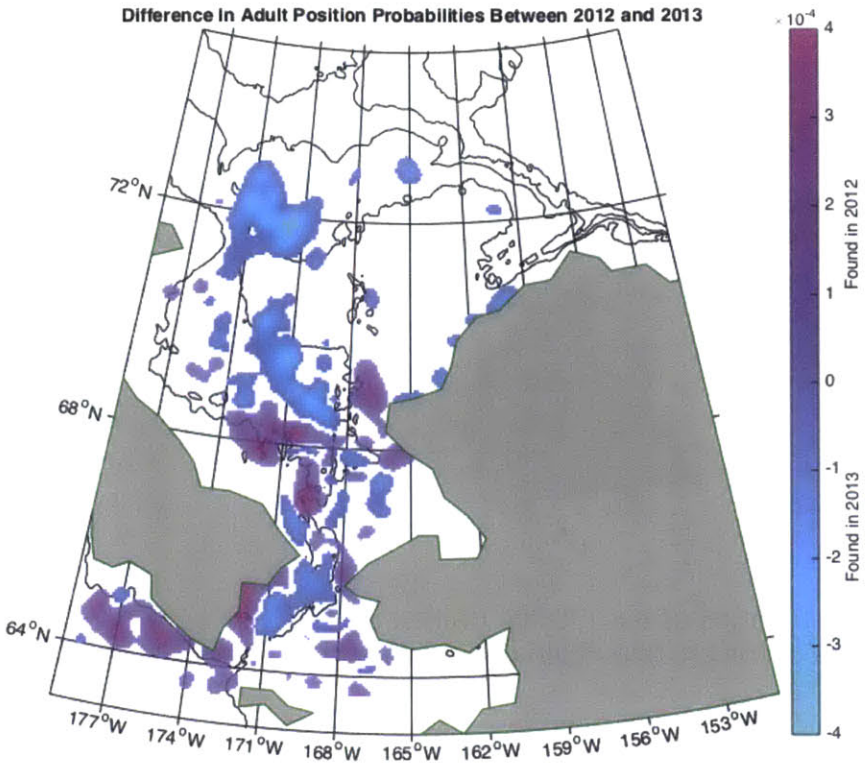

Figure 4-13: The difference between the adult distributions on 3 March from the 2012 and 2013 primary source experiments. The result for 2013 was subtracted from the 2012 result and all values greater than 5x10-5 were retained.

4.6 Sensitivity to Depth of Release

4.6.1 Sink Experiments

The distributions of copepods at the end of the sink experiments were highly sensitive to the depths at which they were released. In general deep particles travel further than shallow particles, but there were differences between years. In 2012, deep model copepods composed the majority of the distributions at the east and west extremes of the total distribution (Figure 4-14). Although the particles close to the Alaskan coast were exclusively shallow, the concentration on the shelfbreak appeared to be a mixture of both deep and shallow copepods. The strong dipole just to the west of Barrow Canyon is notable for its uniqueness.

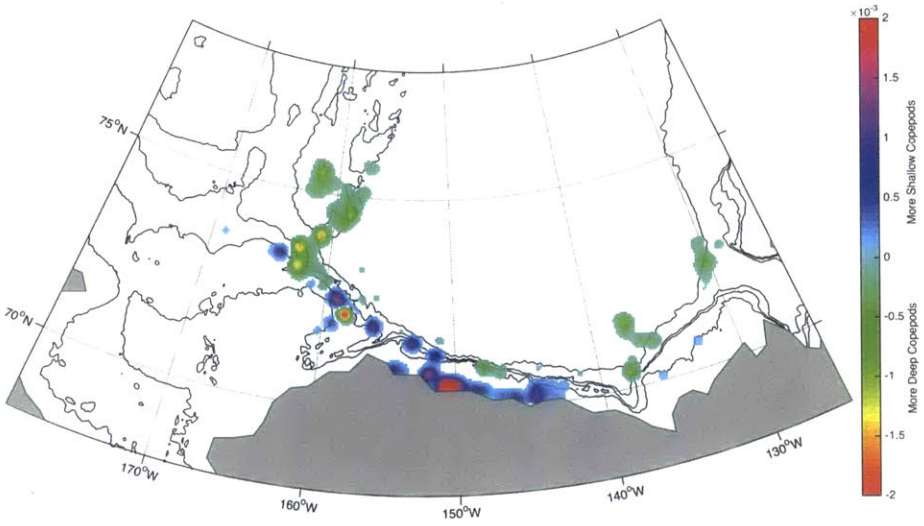

Figure 4-14: The distribution of the 130,000 deepest copepods on 15 December 2012 subtracted from the distribution of the 130,000 shallowest copepods on 15 December 2012.

In 2013, the copepods that traveled furthest east (Fig. 4-15) had more deep constituents than shallow ones. It appears that the shallow copepods that ended up on the Alaskan coast in 2012 ended up on top of the Chukchi Cap in 2013, traveling further west than any of the deep copepods. Deep copepods are still prominent along the western edge of the Canada Basin and on the western edge of Barrow Canyon. Instead of a dipole, we see a larger peak of deep copepods surrounded by regions dominated by shallower copepods.

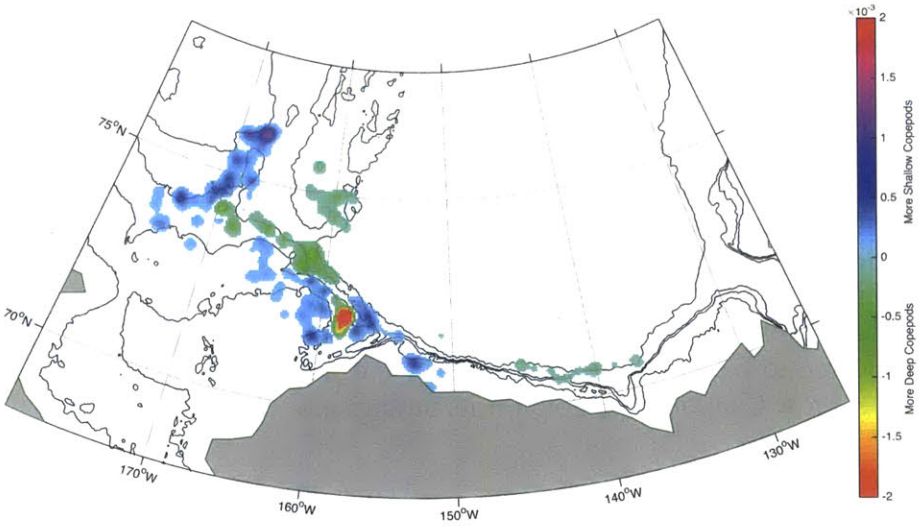

Figure 4-15: The distribution of the 130,000 deepest copepods on 15 December 2013 subtracted from the distribution of the 130,000 shallowest copepods on 15 December 2013.

4.6.2 Source Experiments

In 2012 deep adult copepods tended to start their growing season to the west of shallow copepods with the very notable exception of a large number of adult copepods that started at the base of the central channel just off Cape Lisburne (Figure 4-16). Shallow copepods were concentrated in three regions: the northern entrance to Norton Sound, the southern entrance to Kotzebue Sound and the northern entrance to Kotzebue Sound. The less divergent 2012 distribution of egg release sites is divided into two coherent regions when depth of release is considered. Deep copepods are released in a region connecting eastern Hanna Shoal with the Central Channel while the shallow copepods are released over the broad slope connecting Herald Canyon with Hanna Shoal.

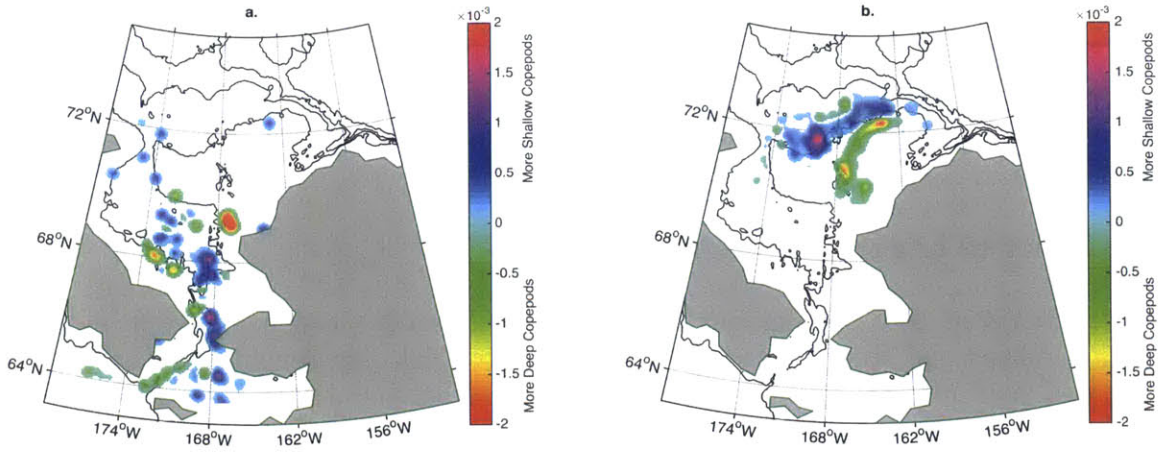

Figure 4-16: The distribution of the 130,000 deepest copepods on 3 March 2012 subtracted from the distribution of the 130,000 shallowest copepods on 3 March 2012 for a) adult copepods and b) egg release locations.

In 2013 the differences between the adult distributions of deep and shallow copepods are much more coherent (Figure 4-17). The shallow copepods started further south from a region that links the Bering Strait with the entrance to Herald Canyon. The deep copepods started in Herald Canyon and on the broad slope that connects the canyon with Hanna Shoal. The differences between the egg release site distributions are very similar to 2012 except that the deep copepods are concentrated in two locations instead of the broader swath seen in 2012 and conversely the shallow copepods are in a broader swath than they were in 2012.

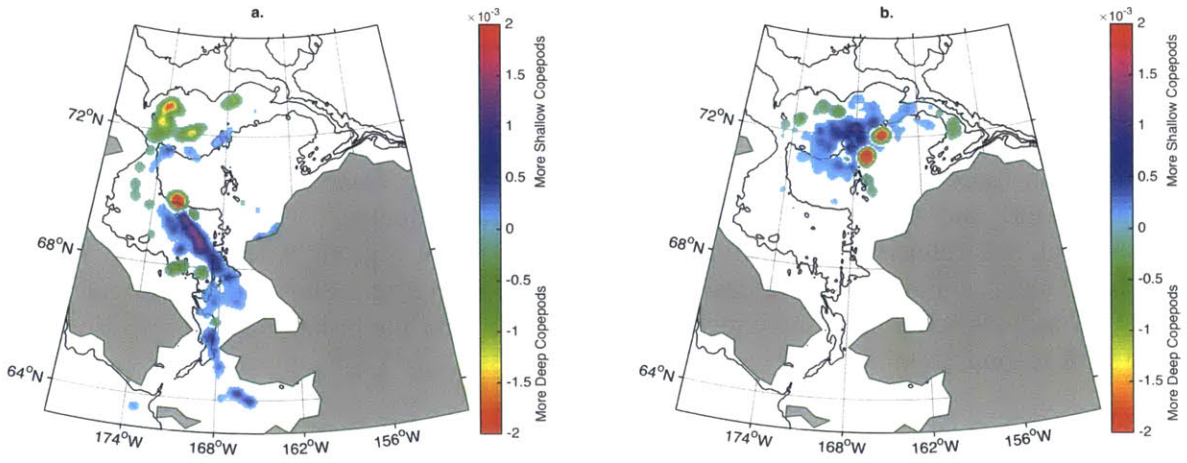

Figure 4-17: The distribution of the 130,000 deepest copepods on 3 March 2013 subtracted from the distribution of the 130,000 shallowest copepods on 3 March 2013 for a) adult copepods and b) egg release locations.

4.7 Sensitivity to Location of Release

Differences between the distributions of the terminal model copepods from the spatial perturbation means and from the results of each source/sink experiment were calculated as indications of how perturbations in spatial distributions that could not be modeled using the model grid sizes might impact the resulting conclusions regarding sources and sinks. For the 2012 sink experiment, the spatial perturbation mean is greater than the primary experiment along the southeastern buttress of the Chukchi Cap and in the region halfway between Barrow and the Canadian Border (Fig. 4-18). These are the same regions where the 2012 distribution was found to be stronger than the 2013 distribution (Fig. 4-11). The differences between the 2013 sink experiment and its corresponding spatial perturbation mean (Fig. 4-19) are much less coherent and smaller in magnitude than the differences observed in 2012.

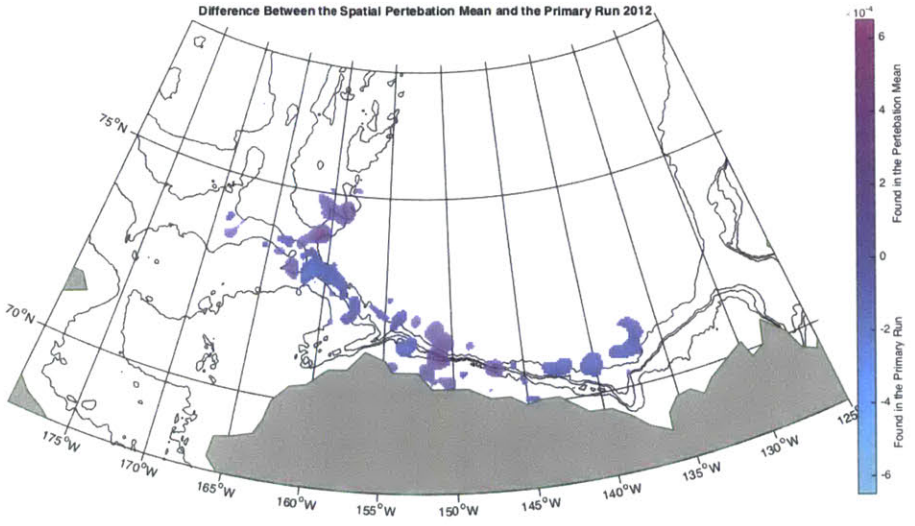

Figure 4-18: Difference between 2012 sink experiment and its corresponding spatial perturbation mean with all values greater than $5x10^{-5}$ retained.

The differences between the other experiments and their corresponding spatial perturbation means are much less coherent and smaller in magnitude than the differences observed in the 2012 sink experiment. The comparison of the 2013 egg release distribution with its corresponding spatial mean is representative of this (Figure 4-19).

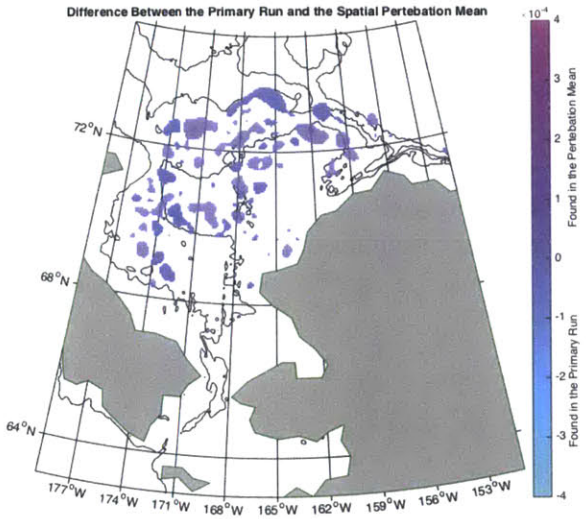

Figure 4-19: Difference between the 2013 egg release site distribution and its corresponding spatial perturbation mean with all values greater than $5x10^{-5}$ retained.

4.8 Sensitivity to Time of Release

The difference between the 2012 sink experiment and its corresponding temporal perturbation mean (Fig. 4-20) is very similar to the corresponding difference observed for the spatial perturbation mean (Fig. 4-18). The southeastern buttress of the Chukchi Cap and in the region halfway between Barrow and the Canadian Border stands out as being more greatly impacted by the temporal perturbations. Again, these are locations where more model copepods terminated in 2012 than in 2013. The temporal perturbations had a lesser impact on the results of the 2013 sink experiment.

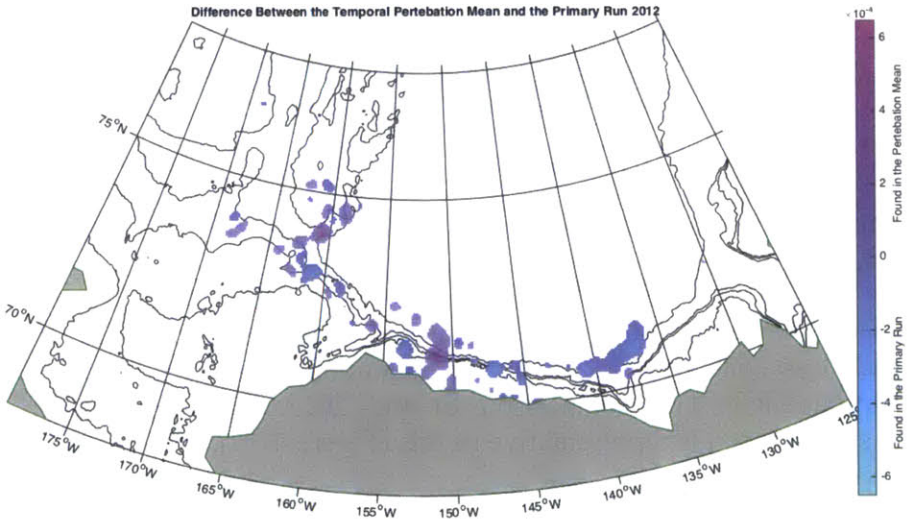

Figure 4-20: Difference between 2012 sink experiment and its corresponding temporal perturbation mean with all values greater than $5x10^{-5}$ retained.

The differences between the other experiments and their corresponding temporal perturbation means are much less coherent and smaller in magnitude than the differences observed in the 2012 sink experiment. The comparison of the 2013 adult source distribution with its corresponding temporal mean is representative of this (Figure 4-21).

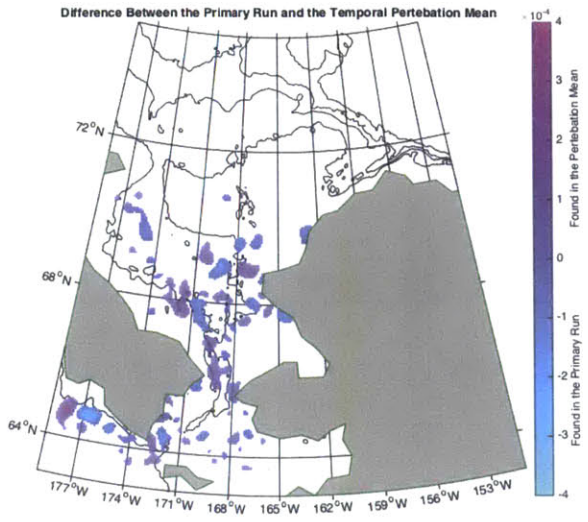

Figure 4-21: Difference between the 2012 adult source distribution and its corresponding temporal perturbation mean with all values greater than $5x10^{-5}$ retained.

4.9 Statistical Treatment of Sensitivity and Interannual Differences

The previous sections graphically reviewed the sensitivity of the source and sink distributions to depth, position and time of release as well as the interannual differences between the experiments. Here we will examine the results of the statistical analysis conducted in an attempt to quantify these differences.

The calculated interannual variation for the sink experiment was 0.4929, more than twice the variation calculated between the primary experiment for either year and either of their corresponding perturbation means (Table 4.1). The calculated interannual variation for the source experiment distributions of adults was 0.5458, more than twice the variation calculated between the primary experiment for either year and either of their corresponding perturbation means (Table 4.1). The calculated interannual variation for the source experiment distributions of egg release sites was 0.2172, more than twice the variation calculated between the primary experiment for either year and either of their corresponding perturbation means (Table 4.1).

Table 4.1: Center of mass (CoM) distances in kilometers.

Year	Perturbation	Experiment	Class	Variation	CoM North	CoM South	CoM East	CoM West	CoM
2012	Spatial	Sink	All	0.1983	-	-	75.617	20.765	-
2013	Spatial	Sink	All	0.1388	-	-	24.987	8.722	-
2012	Spatial	Source	Egg	0.0654	-	-	-	-	1.076
2013	Spatial	Source	Egg	0.0849	-	-	-	-	7.014
2012	Spatial	Source	Adult	0.2437	7.239	3.042	-	-	-
2013	Spatial	Source	Adult	0.2435	14.710	17.844	-	-	-
2012	Temporal	Sink	All	0.1709	-	-	80.113	3.808	-
2013	Temporal	Sink	All	0.1174	-	-	50.373	35.224	-
2012	Temporal	Source	Egg	0.0594	-	-	-	-	2.077
2013	Temporal	Source	Egg	0.0784	-	-	-	-	1.549
2012	Temporal	Source	Adult	0.2105	20.813	17.125	-	-	-
2013	Temporal	Source	Adult	0.202	9.1312	14.07	-	-	-

In 2013, the center of mass of the eastern hotspot of the sink distribution moved 161.7 km to the east from its position in 2012. This is more than twice the distance between eastern centers of mass in the sink experiment for either year and either of their corresponding perturbation means (Table 4.1). In 2013 the center of mass of the western hotspot of the sink distribution moved 36.7 km to the west from it position in 2012. This is roughly the same distance between western center of mass in the sink experiment for 2013 its corresponding temporal perturbation mean (Table 4.1). It is only slightly larger than the distance between western center of mass in the sink experiment for 2012 and its corresponding spatial perturbation mean (Table 4.1).

In 2013 the center of mass of the hotspot of the egg release distribution moved 13.5 km to the northwest from its position in 2012. This is almost twice the distance between egg release centers of mass in the source experiment for either year and either of their corresponding perturbation means (Table 4.1). In 2013, the center of mass of the northern hotspot of the adult distribution moved 139.5 km to the north from its position in 2012. This is more than six times the distance between northern centers of mass in the source experiment for either year and either of their corresponding perturbation means (Table 4.1). In 2013, the center of mass of the southern hotspot of the adult distribution moved 179.6 km to the east from its position in 2012. This is more than ten times the distance between southern centers of mass in the source experiment for either year and either of their corresponding perturbation means (Table 4.1).

There is no clear indication of the solution being more sensitive to temporal or spatial perturbations. In 2012 the temporal distances are longer in three out of the five cases. In 2013 the exact opposite pattern is seen with the spatial distances being longer in the same three out of five cases (Table 4.1).

With the exception of one case, the slip and slid method never reduced the variation between solutions by more than 14% and typical reductions were less than 10% (Table 4.2). In general

they confirm the results of the center of mass analysis in that the interannual variation is more significant than the variations between primary experiments and their perturbation means.

Table 4.2: Sink experiment slip and slide analysis.

Experiment	Perturbation	Year	East		West	
			Initial	Slip/Slide	Initial	Slip/Slide
24	Spatial	2012	0.3454	0.3289	0.1829	0.1734
25	Spatial	2013	0.4351	0.4095	0.1329	0.1278
24	Temporal	2012	0.3019	0.2967	0.1387	0.1327
25	Temporal	2013	0.4588	0.4249	0.1114	0.1088
3 to 6	Spatial	2012	0.1314	0.1235	0.0719	0.0711
6 to 12	Spatial	2012	0.0593	0.0587	0.0241	0.0239
3 to 6	Temporal	2012	0.0948	0.092	0.0456	0.0448
6 to 12	Temporal	2012	0.0534	0.531	0.0307	0.0305
24-25	Interannual	2012-2013	0.867	0.232	0.471	0.4302
25-24	Interannual	2013-2012	0.867	0.7535	0.471	0.4662

The method is sometimes very sensitive the direction of comparison, in other words which hotspot is manipulated to fit the other. This is seen when the method was applied to the 2012 and 2013 eastern sink hotspots (Table 4.2). This one case where variation was reduced by almost 75% involved extreme, unrealistic manipulation. The 2012 eastern sink hotspot was compressed by a factor of 2 in the x direction and stretched by a factor of 6 in the y direction. The fact that the variation as modified by slip and slide appears to be less than the variations as modified by slip and slide observed when comparing primary experiments with their perturbation means should be disregarded for this reason.

Again, with the exception of one case, when applied to the source experiment, the slip and slid method never reduced the variation between solutions by more than 14% and typical reductions were less than 10% (Table 4.3). They further confirm the results of the center of mass analysis in that the interannual variation is always at least twice the variations between primary experiments and their perturbation means.

When we compare a mean of three perturbations to a mean of six perturbations, we see that the variation is less than half the variation yielded by the comparison of a primary experiment with a three-perturbation mean (Table 4.2). When we compare a mean of six perturbations to a mean of twelve perturbations in the spatial case, the variation is less than half the variation yielded by the comparison between three and six perturbations. In the temporal case, the six to twelve perturbation comparison yields variation that is slightly more than half the variation yielded by the comparison between three and six perturbations. This implies that the spatial perturbations are converging faster than the temporal perturbations, but it is important to recognize that the variation in the temporal case was already generally lower than the variation in the spatial case. This analysis suggests that using more perturbations would have resulted in a mean closer to the true mean, however, the fact that the variation is converging means that we can be confident that our three perturbation means are representative of the true means, they just contain more error.

Since this error with only three perturbations is still much less than the interannual differences we identified, our three perturbation means are sufficient.

Table 4.3: Source experiment slip and slide analysis.

Experiment	Perturbation	Year	Eggs	
			Initial	Slip/Slide
24	Spatial	2012	0.1123	0.1074
25	Spatial	2013	0.1434	0.1409
24	Temporal	2012	0.0786	0.0753
25	Temporal	2013	0.0972	0.0951
24-25	Interannual	2012-2013	0.4323	0.3584
25-24	Interannual	2013-2012	0.4323	0.3826

Experiment	Perturbation	Year	Adults-North		Adults-South	
			Initial	Slip/Slide	Initial	Slip/Slide
24	Spatial	2012	0.2889	0.2812	0.2991	0.2941
25	Spatial	2013	0.3165	0.3117	0.335	0.3295
24	Temporal	2012	0.2867	0.2783	0.2947	0.2876
25	Temporal	2013	0.2818	0.2658	0.2859	0.272
24-25	Interannual	2012-2013	0.6772	0.6741	0.6985	0.614
25-24	Interannual	2013-2012	0.6772	0.6621	0.6985	0.6837

Chapter 5

Discussion

5.1 Identification of *C. glacialis* Source and Sink Regions for Hanna Shoal

Our work shows that *C. glacialis* that have achieved copepodid stage one over the highly productive Hanna Shoal region by August will have the potential to mature to a diapause competent stage before the severe food shortage of the Arctic fall drastically reduces their growth potential. These copepods do not remain over Hanna Shoal, but instead within two months are advected off the shoal, generally through Barrow Canyon. After entering the Beaufort Sea, some travel east in the shelfbreak jet while others travel west in the countercurrent. Hanna Shoal appears to have the potential to be connected with both the *C. glacialis* population entering diapause over the Beaufort Shelf and the population entering diapause over the southeastern corner of the Chukchi Cap. The relative strength of this connection changes on an interannual basis.

We show that *C. glacialis* copepodids observed over Hanna Shoal in August are likely less than two months old and although they did not start their lives over the Shoal, they were released by their mothers within 450 km of it. Given the relatively short amount of time they have had to be advected, it is unsurprising that the distribution of their starting positions is a single cohesive region. This source region is centered at the northern end of the Central Channel and appears to include eggs released by adults moving northeast after exiting Herald Canyon as well as adults traveling through Central Channel itself. Although the shape and the center of mass of this distribution does change interannually, the differences are slight and do not appear to be very meaningful.

Adults over Hanna Shoal have a much less cohesive distribution of their starting locations on 3 March; it is stretched over 1500 km from the southwest corner of the Beaufort Sea to the Gulf of Anadyr. Between one quarter and one third of the adults start south of the Bering Strait. This southern source region strongly favors the Gulf of Anadyr over Norton Sound. This is likely due to the greater strength of the Anadyr Current relative to the Alaskan Coastal Current. Through a similar experiment using an IBM, Bérline et al. (2008) found that euphausiids in the vicinity of Barrow could have origins either in the Anadyr Gulf or in the Shpanberg Strait at the mouth of Norton Sound, however the authors did not try to evaluate the relative importance of these source regions. In the present study, the northern source region is fragmented between individuals in three different pathways: Herald Canyon to the west, the Alaskan coast to the east and Central Channel in the middle. The vertical compression or extension of this northern source region appears to vary significantly from year to year. It is important to note that in 2012 not a single

adult came from the Beaufort Sea, while in 2013 a very small proportion did come from the Beaufort Sea.

The lack of significant overlap between the source and sink regions in the Chukchi underlines an important reality for this Arctic shelf species. The populations over the northern Chukchi do not appear to have the physical potential to be self-sustaining, instead they are dependent on transients, mainly from southern populations. *C. glacialis* individuals have been observed reproducing in the Beaufort Sea (Plourde et al., 2005) and the Beaufort Gyre provides an advective environment that would allow self-sustainment assuming individuals can survive periods in the central Arctic. Observations of healthy *C. glacialis* at 80°N (Ashjian et al., 2003; Nelson et al., 2009) suggest this is the case.

Genetic work conducted by Nelson et al. (2009) on *C. glacialis* sampled in July 2002 from the Chukchi Sea and Arctic Ocean identified two dominant haplotypes: a North Pacific/Bering type and an Arctic type. This indicates that *C. glacialis* at the northern extent of its range is able to sustain itself without contributions from the south. They found the Chukchi Sea to be dominated by the southern haplotype as would be suggested by our source experiment. As expected, they found southern haplotype amongst *C. glacialis* populations over the southern Chukchi Cap as would be suggested by our sink experiment, but interestingly their two sites over the Beaufort Shelf hosted only the northern haplotype. This could mean that southern expatriates advected to this sink region do not survive, however Nelson et al.'s low sampling resolution leaves open the possibility that they just missed the southern expatriates. Genetic work conducted by R. Campbell (pers. comm) over multiple years in the Chukchi and Beaufort Sea and in 2012 and 2013 on Hanna Shoal as part of this project also demonstrated that the southern haplotype dominates in the Chukchi Sea and that the northern (Arctic) haplotype is present only in Beaufort Sea and Canada Basin to the north, along the Chukchi Sea shelfbreak and on the northern edge of Hanna Shoal, or where significant southward advective events in Barrow Canyon have brought Arctic haplotypes south.

5.2 Importance of Physical Control on the Distribution

Although the daily mean currents provided by AO-FVCOM were highly variable over the course of the month, copepods in these experiments moved more or less in line with the monthly mean conditions. The generally consistent northward currents with very little recirculation place severe limits on long-lived plankton such as *C. glacialis* by restricting the regions with which each population is connected. The physical conditions set the maximum limits of the source and sink regions, while predation, mortality and food conditions will result in source and sink regions that are a subset of these regions.

In this set of experiments, several specific physical oceanographic features were found to have outsize impacts on determining the upstream and downstream connections of Hanna Shoal with other regions. In the sink experiment, the Barrow Canyon outflow was of utmost importance. In the source experiment the Bering Strait inflow and outflow played a defining role.

Very few copepods left Hanna Shoal without passing through Barrow Canyon; they followed the clockwise circulation around the shoal until they were entrained in the energetic outflow. The junction between the outflow and the shelfbreak current proved to be a particularly deterministic

point in their journey. The AO-FVCOM represented this point as a particularly strong vorticity dipole with strong positive vorticity on the west side and negative vorticity on the east side. Pickart et al. (2005) explain that this feature results from the incomplete adjustment of water exiting the canyon as it sinks, stretches and decelerates. The exact position of a copepod relative to this feature would determine whether it would be found in east or west hotspot. Five kilometers of difference at this point between two copepods could result in over 800 km of difference between the same two copepods on December 15th. This feature is clearly not an artifact of the model as similar behavior has been observed in drifters released over the Chukchi Sea.

Adult copepods arrived over Hanna Shoal following one of three routes, Herald Canyon, Central Channel and the Alaskan Coastal Current. The tendency of the Bering Strait outflow to favor the western route led the Herald Canyon to be the most important of the three. The strength of the Anadyr Current as it enters Bering Strait limits the flow into the Strait from Norton Sound and the region east of St. Lawrence Island. If copepods were released at the same latitude in Norton Sound and the Anadyr Gulf, those released in the Anadyr Gulf would be hundreds of kilometers further north by the beginning of August.

While the exact time and location of release had fairly minimal effect on the locations of the source and sink regions, relatively small differences in depth of release had strong effects on both starting positions at the end of the source experiment and ending positions at the end of the sink experiment. This is due to the importance of topographic steering that results from the shallow nature of the Chukchi. Bérline et al. (2008) found that euphausiids released near the bottom in the Anadyr Gulf and Shpanberg Strait were more concentrated in Barrow canyon than those released near the surface. In our scenario, although their trajectories were different, the deep copepods were no more concentrated than the shallow copepods (Figures 4-14 and 4-15). Interestingly enough in our source experiment, we found that the furthest travelling shallow copepods were more likely to come from the vicinity of Shpanberg Strait, while the furthest travelling deep copepods were more likely to come from Anadyr Gulf (Figures 4-16 and 4-17).

5.3 Potential Impacts of Environmental Calamities

The importance of Hanna Shoal as a way station on the route from almost the entire Chukchi Sea to the Beaufort Sea and Chukchi Cap means that any sort of catastrophic event in this region, such as an oil spill, would have severe follow-on effects on much of the western Arctic. Even if the direct impacts were limited to the shoal only, the populations of bowhead whales and other western Arctic marine mammals that depend on zooplankton for food would suffer greatly while migrating through the region. In addition, very little zooplankton stock would be exported to the Beaufort Sea and Chukchi Cap from the Chukchi Sea. Even if these zooplankton are not important in terms of self-sustainment of the Arctic *C. glacialis* stock, they represent a substantial flux of energy, if only as lipid filled carcasses (Daase et al., 2014).

In addition to predicting the scope of an environmental calamity on *C. glacialis,* our results could also be interpreted to tell us something about the fate of a pollutant itself, if released in our area of interest. Although models that directly incorporate weathering, such as the Oil-Spill Risk Analysis (OSRA) model used by BOEM exist to predict the outcome of potential oil spills (BOEM, 2015), the quality of the forcing we used in this work and detailed analysis presented

here warrant investigation. The source regions could be interpreted as areas where an oil spill would have a high probability of impacting Hanna Shoal itself and the sink regions could be interpreted as areas that would be impacted following an oil spill over Hanna Shoal. With additional parameterization, FISCM could be adapted to account for weathering as well as the differences in the physics of advecting the different components of oil. Results could then be directly compared to output generated by OSRA or they could be combined to create an ensemble prediction.

As discussed in Chapter 2, the impacts of climate change on the distribution of *C. glacialis* remain poorly understood. Our results do add more context to the work surrounding this question. For example, if more phytoplankton biomass is available the Anadyr Gulf it is reasonable to believe that the population of *C. glacialis* would benefit, although its competitive interactions with northward moving southern competitors would have to be studied. This might result in more mature adults being exported into the Chukchi and in turn more diapause competent individuals being exported to the Beaufort Sea and Chukchi Cap. What remains unlikely is these southern haplotype *C. glacialis* becoming self-sustaining as their offspring would rarely get the chance to feed and develop in the food rich, relatively warm Chukchi.

5.4 Assumptions and Limitations

The number of assumptions inherent in our work limits the impact of our conclusions. Similarly to Ji et al.'s (2012) work, we assume that AO-FVCOM output represents the real current field and we neglect food limitations, mortality and depth varying behavior. We have every reason to believe that the modeled current regime provided by AO-FVCOM is a reasonable approximation of the actual currents in our domain. The diel vertical migration behavior of Arctic species is highly affected by daylight cycles in the Arctic and is not fully understood. Thus, the behavior is difficult to replicate in a model. By locking our copepods in their release depth we lose a degree of detail, as we know the depth has a measureable effect on source and sink distributions. The assumptions relative to food and mortality mean different things in the sink and source experiments.

The sink experiment shows the maximum extent of the early winter distribution of the *C. glacialis* that were observed over Hanna Shoal in August. This means we can be reasonably sure that any regions outside the reported distribution are not supplied by *C. glacialis* from Hanna Shoal. The fact that we did not model mortality means that the true distribution of *C. glacialis* from Hanna Shoal is actually smaller than we reported. One example is the discrepancy between observational studies, which have not found *C. glacialis* close to shore on the Beaufort Shelf and our 2012 results that show a large concentration of *C. glacialis* from Hanna Shoal very close to shore.

The distributions generated by the source experiment have a different set of limitations. Our distribution tracks copepods that we know survived, but we have no idea how many copepods were present in the source regions when they started moving. This means that a strong concentration in our source distribution could be because there was a corresponding peak in the *C. glacialis* distribution in that region on 3 March or it could be because *C. glacialis* from that region suffered less mortality than other regions as they progressed to Hanna Shoal. This means if a putative source region were to suffer a decline in *C. glacialis* abundance we would expect

Hanna Shoal to suffer, but if a putative source region had an increase in *C. glacialis* abundance we cannot expect Hanna Shoal to benefit as mortality dynamics might prevent the additional copepods from reaching Hanna Shoal.

Our treatment of diffusion also represents a series of assumptions. By simply passing a filter over the distribution at the end, we are assuming that each release point serves as the center of a 2-D normal distribution with fixed dimensions that is advected and developed only by the conditions found in the center. In a more realistic simulation, the distribution would slowly diffuse over time. The edges of this more realistic distribution would be affected differently than the center due to spatial variability of currents and water temperatures and the final solution at the end of the simulation would look different. We mitigated the limitations imposed by our assumptions by using perturbation analysis. If the differences in forcing between the center and the edges of our distributions fundamentally changed the solution it would have manifested itself in a much larger difference between our perturbation mean and our primary experiment solution. Although this was not the case, it would be interesting in the future to directly compare the results of perturbation analysis using FISCM with different implementations of horizontal diffusivity using the same model.

Chapter 6

Conclusion

This work clearly shows the promise of the thoughtful synthesis of observational work and modeling efforts in investigating biophysical interactions. Using modeling techniques, the implications of observations can be tested. Likewise by coupling models to observation, fewer assumptions are made and results are inherently more meaningful. Of course the quality of output will always be linked to the resolution of the model used and the resolution of the observational data with which it is coupled. With more data and higher resolution model output, even more nuanced investigation could be made.

Arctic research is difficult and expensive, but to test the assertion of source and sink regions, it would be excellent to sample the putative source regions early in the spring, across the Chukchi in midsummer and the putative sink regions in the Beaufort in early fall. Such an experiment linked with additional modeling could allow us to at least partially detangle the impacts of the physical and biological factors that determine the size of the *C. glacialis* population at any given point. This sort of sequential sampling effort could be coupled with the modeling of numerous different species of zooplankton, although extending beyond copepods would likely require extensive laboratory work ex-situ in order to properly parameterize the other taxa in an IBM such as FISCM.

Temperature and salinity are conservative properties that are commonly used in physical oceanography to track water masses. Zooplankton are not conservative at all, but they could be imagined as integrative tracers that pass important information about the physical and biological conditions they have encountered as they are advected through a domain. As our ability to model zooplankton and their interactions with the environment improves, perhaps in the future we could approach this from a completely different direction. By assuming a deterministic distribution of zooplankton across a domain we could model the simplest physical conditions that resulted in such a distribution.

Bibliography

von Appen, W.-J., & Pickart, R. S. (2012). Two Configurations of the Western Arctic Shelfbreak Current in Summer. *Journal of Physical Oceanography*, 42(3), 329–351. http://doi.org/10.1175/JPO-D-11-026.1

Arrigo, K. R., Perovich, D. K., Pickart, R. S., Brown, Z. W., van Dijken, G. L., Lowry, K. E., et al. (2014). Phytoplankton blooms beneath the sea ice in the Chukchi Sea. *Deep-Sea Research Part II*, 105(C), 1–16. doi:10.1016/j.dsr2.2014.03.018

Ashjian, C. J., Campbell, R. G., Welch, H. E., Butler, M., & Van Keuren, D. (2003). Annual cycle in abundance, distribution, and size in relation to hydrography of important copepod species in the western Arctic Ocean. *Deep Sea Research Part I: Oceanographic Research Papers*, 50(10-11), 1235–1261. doi:10.1016/S0967-0637(03)00129-8

Ashjian, C. J., Gallager, S. M., & Plourde, S. (2005). Transport of plankton and particles between the Chukchi and Beaufort Seas during summer 2002, described using a Video Plankton Recorder. *Deep Sea Research Part II: Topical Studies in Oceanography*, 52(24-26), 3259–3280. doi:10.1016/j.dsr2.2005.10.012

Balch, W. M., Bowler, B. C., Lubelczyk, L. C., & Stevens, M. W. (2014). Aerial extent, composition, bio-optics and biogeochemistry of a massive under-ice algal bloom in the Arctic. *Deep Sea Research Part II: Topical Studies in Oceanography*, 105(C), 42–58. doi:10.1016/j.dsr2.2014.04.001

Bérline, L., Spitz, Y. H., Ashjian, C. J., Campbell, R. G., Maslowski, W., & Moore, S. E. (2008). Euphausiid transport in the Western Arctic Ocean. *Marine Ecology Progress Series*, 360, 163–178. http://doi.org/10.3354/meps07387

Bureau of Ocean Energy Management (BOEM). (2015). *Environmental Studies Program.* Retrieved from http://www.boem.gov/Studies

Brown, Z. W., Lowry, K. E., Palmer, M. A., van Dijken, G. L., Mills, M. M., Pickart, R. S., & Arrigo, K. R. (2015). Characterizing the subsurface chlorophyll a maximum in the Chukchi Sea and Canada Basin. *Deep Sea Research Part II: Topical Studies in Oceanography*, 1–17. doi:10.1016/j.dsr2.2015.02.010

Brugler, E. T., Pickart, R. S., Moore, G. W. K., Roberts, S., Weingartner, T. J., & Statscewich, H. (2014). Seasonal to interannual variability of the Pacific water boundary current in the Beaufort Sea. *Progress in Oceanography*, 127(C), 1–20. http://doi.org/10.1016/j.pocean.2014.05.002

Campbell, R. G., Sherr, E. B., Ashjian, C. J., Plourde, S., Sherr, B. F., Hill, V., & Stockwell, D. A. (2009). Mesozooplankton prey preference and grazing impact in the western Arctic Ocean. *Deep Sea Research Part II: Topical Studies in Oceanography*, 56(17), 1274–1289. doi:10.1016/j.dsr2.2008.10.027

Campbell, R., Wagner, M., Teegarden, G., Boudreau, C., & Durbin, E. (2001). Growth and development rates of the copepod Calanus finmarchicus reared in the laboratory. *Marine Ecology Progress Series*, 221, 161-183.

Chen, C., Beardsley, R. C., Cowles, G., & Qi, J. (2013a). *An Unstructured Grid, Finite-Volume Community Ocean Model: FVCOM User Manual.* New Bedford, MA: Marine Ecosystem Dynamics Modeling Laboratory.

Chen, C., Gao, G., Qi, J., Proshutinsky, A., Beardsley, R. C., Kowalik, Z., et al. (2009). A new high-resolution unstructured grid finite volume Arctic Ocean model (AO-FVCOM): An application for tidal studies. *Journal of Geophysical Research*, 114(C8), C08017–20. http://doi.org/10.1029/2008JC004941

Chen, H., Wang, H., Shu, Q., Wang, D., & Liu, N. (2013b). Ocean current observation and spectrum analysis in central Chukchi Sea during the summer of 2008. *Acta Oceanologica Sinica*, 32(3), 10–18. http://doi.org/10.1007/s13131-013-0283-7

Daase, M., Falk-Petersen, S., Varpe, Ø., Darnis, G., Søreide, J. E., Wold, A., et al. (2013). Timing of reproductive events in the marine copepod Calanus glacialis: a pan-Arctic perspective. *Canadian Journal of Fisheries and Aquatic Sciences*, 70(6), 871–884. doi:10.1139/cjfas-2012-0401

Daase, M., Varpe, O., & Falk-Petersen, S. (2014). Non-consumptive mortality in copepods: occurrence of Calanus spp. carcasses in the Arctic Ocean during winter. *Journal of Plankton Research*, 36(1), 129–144. http://doi.org/10.1093/plankt/fbt079

Danielson, S. L., Weingartner, T. J., Hedstrom, K. S., Aagaard, K., Woodgate, R., Curchitser, E., & Stabeno, P. J. (2014). Coupled wind-forced controls of the Bering-Chukchi shelf circulation and the Bering Strait throughflow: Ekman transport, continental shelf waves, and variations of the Pacific-Arctic sea surface height gradient. *Progress in Oceanography*, 125(C), 40–61. doi:10.1016/j.pocean.2014.04.006

Day, R. H., Weingartner, T. J., Hopcroft, R. R., Aerts, L. A. M., Blanchard, A. L., Gall, A. E., et al. (2013). The offshore northeastern Chukchi Sea, Alaska: A complex high-latitude ecosystem. *Continental Shelf Research*, 67(C), 147–165. doi:10.1016/j.csr.2013.02.002

Falk-Petersen, S., Mayzaud, P., Kattner, G., & Sargent, J. R. (2009). Lipids and life strategy of Arctic Calanus. *Marine Biology Research*, 5(1), 18–39. doi:10.1080/17451000802512267

Genin, A. (2004). Bio-physical coupling in the formation of zooplankton and fish aggregations over abrupt topographies. *Journal of Marine Systems*, 50(1-2), 3–20. doi:10.1016/j.jmarsys.2003.10.008

Gao, G., Chen, C., Qi, J., & Beardsley, R. C. (2011). An unstructured-grid, finite-volume sea ice model: Development, validation, and application. *Journal of Geophysical Research*, 116, C00D04–15. http://doi.org/10.1029/2010JC006688

Genin, A. (2004). Bio-physical coupling in the formation of zooplankton and fish aggregations over abrupt topographies. *Journal of Marine Systems*, 50(1-2), 3–20. http://doi.org/10.1016/j.jmarsys.2003.10.008

Gentleman, W. C., Neuheimer, A. B., & Campbell, R. G. (2008). Modelling copepod development: current limitations and a new realistic approach. *ICES Journal of Marine Science: Journal Du Conseil*, 65(3), 399–413. doi:10.1093/icesjms/fsn047

Gong, D., & Pickart, R. S. (2015). Summertime Circulation in the Eastern Chukchi Sea. *Deep Sea Research Part II: Topical Studies in Oceanography*, 1–51. doi:10.1016/j.dsr2.2015.02.006

Hill, V., Cota, G., & Stockwell, D. (2005). Spring and summer phytoplankton communities in the Chukchi and Eastern Beaufort Seas. *Deep Sea Research Part II: Topical Studies in Oceanography*, 52(24-26), 3369–3385. http://doi.org/10.1016/j.dsr2.2005.10.010

Hopcroft, R. R., & Day, R. H. (2013). Introduction to the special issue on the ecology of the northeastern Chukchi Sea. *Continental Shelf Research*, 67(C), 1–4. http://doi.org/10.1016/j.csr.2013.06.017

Hopcroft, R. R., Kosobokova, K. N., & Pinchuk, A. I. (2010). Zooplankton community patterns in the Chukchi Sea during summer 2004. *Deep Sea Research Part II: Topical Studies in Oceanography*, 57(1-2), 27–39. doi:10.1016/j.dsr2.2009.08.003

Hunt, G. L., Jr., Blanchard, A. L., Boveng, P., Dalpadado, P., Drinkwater, K. F., Eisner, L., et al. (2013). The Barents and Chukchi Seas: Comparison of two Arctic shelf ecosystems. *Journal of Marine Systems*, 109-110, 43–68. doi:10.1016/j.jmarsys.2012.08.003

Ji, R., Ashjian, C. J., Campbell, R. G., a, C., Gao, G., Davis, C. S., et al. (2012). Life history and biogeography of Calanus copepods in the Arctic Ocean: An individual-based modeling study. *Progress in Oceanography*, 96(1), 40–56. doi:10.1016/j.pocean.2011.10.001

Kantha, L. H., & Clayson, C. A. (1994). An improved mixed layer model for geophysical applications. *Journal Of Geophysical Research. Oceans*, *99*(C12), 25235. doi:10.1029/94JC02257

Laney, S. R., & Sosik, H. M. (2014). Phytoplankton assemblage structure in and around a massive under-ice bloom in the Chukchi Sea. *Deep Sea Research Part II: Topical Studies in Oceanography*, 105(C), 30–41. doi:10.1016/j.dsr2.2014.03.012

Lee, S. H., Dahms, H.-U., Kim, Y., Choy, E. J., Kang, S.-H., & Kang, C.-K. (2013). Spatial distribution of small phytoplankton composition in the Chukchi Sea. *Polar Biology*, 37(1), 99–109. doi:10.1007/s00300-013-1413-6

Llinás, L., Pickart, R. S., Mathis, J. T., & Smith, S. L. (2009). Zooplankton inside an Arctic Ocean cold-core eddy: Probable origin and fate. *Deep Sea Research Part II: Topical Studies in Oceanography*, 56(17), 1290–1304. doi:10.1016/j.dsr2.2008.10.020

Lowry, K. E., van Dijken, G. L., & Arrigo, K. R. (2014). Evidence of under-ice phytoplankton blooms in the Chukchi Sea from 1998 to 2012. *Deep Sea Research Part II: Topical Studies in Oceanography*, 105(C), 105–117. doi:10.1016/j.dsr2.2014.03.013

Mathis, J. T., & Questel, J. M. (2013). Assessing seasonal changes in carbonate parameters across small spatial gradients in the Northeastern Chukchi Sea. *Continental Shelf Research*, 67(C), 42–51. doi:10.1016/j.csr.2013.04.041

Matsuno, K., Yamaguchi, A., & Imai, I. (2012). Biomass size spectra of mesozooplankton in the Chukchi Sea during the summers of 1991/1992 and 2007/2008: an analysis using optical plankton counter data. *ICES Journal of Marine Science*, 69(7), 1205–1217. http://doi.org/10.1093/icesjms/fss119

Matsuno, K., Yamaguchi, A., Hirawake, T., & Imai, I. (2011). Year-to-year changes of the mesozooplankton community in the Chukchi Sea during summers of 1991, 1992 and 2007, 2008. *Polar Biology*, 34(9), 1349–1360. doi:10.1007/s00300-011-0988-z

McPhee, M. G. (2013). Intensification of Geostrophic Currents in the Canada Basin, Arctic Ocean. *Journal of Climate*, 26(10), 3130–3138. http://doi.org/10.1175/JCLI-D-12-00289.1

Mellor, G. L., & Yamada, T. (1982). Development of a turbulence closure model for geophysical fluid problems. *Reviews of Geophysics*, 20(4), 851–875. http://doi.org/10.1029/RG020i004p00851

Miller, C. B., Lynch, D. R., & Carlotti, F. (1998). Coupling of an individual based population dynamic model of Calanus finmarchicus to a circulation model for the Georges Bank region. *Fisheries Oceanography*, 7(3/4), 219–234.

Nelson, R. J., Carmack, E. C., McLaughlin, F. A., & Cooper, G. A. (2009). Penetration of Pacific zooplankton into the western Arctic Ocean tracked with molecular population genetics. *Marine Ecology Progress Series*, 381, 129–138. http://doi.org/10.3354/meps07940

Neuheimer, A. B., Gentleman, W. C., Pepin, P., & Head, E. J. H. (2010a). Explaining regional variability in copepod recruitment: Implications for a changing climate. *Progress in Oceanography*, 87(1-4), 94–105. doi:10.1016/j.pocean.2010.09.008

Neuheimer, A. B., Gentleman, W. C., Pepin, P., & Head, E. J. H. (2010b). How to build and use individual-based models (IBMs) as hypothesis testing tools. *Journal of Marine Systems*, 81(1-2), 122–133. doi:10.1016/j.jmarsys.2009.12.009

Neukermans, G., Reynolds, R. A., & Stramski, D. (2014). Contrasting inherent optical properties and particle characteristics between an under-ice phytoplankton bloom and open water in the Chukchi Sea. *Deep Sea Research Part II: Topical Studies in Oceanography*, 105(C), 59–73. doi:10.1016/j.dsr2.2014.03.014

Nikolopoulos, A., Pickart, R. S., Fratantoni, P. S., Shimada, K., Torres, D. J., & Jones, E. P. (2009). The western Arctic boundary current at 152°W: Structure, variability, and transport. *Deep Sea Research Part II: Topical Studies in Oceanography*, 56(17), 1164–1181. http://doi.org/10.1016/j.dsr2.2008.10.014

Norcross, B. L., Raborn, S. W., Holladay, B. A., Gallaway, B. J., Crawford, S. T., Priest, J. T., et al. (2013). Northeastern Chukchi Sea demersal fishes and associated environmental characteristics, 2009–2010. *Continental Shelf Research*, 67(C), 77–95. doi:10.1016/j.csr.2013.05.010

Ortega-Retuerta, E., Fichot, C. G., Arrigo, K. R., Van Dijken, G. L., & Joux, F. (2014). Response of marine bacterioplankton to a massive under-ice phytoplankton bloom in the Chukchi Sea (Western Arctic Ocean). *Deep Sea Research Part II: Topical Studies in Oceanography*, 105(C), 74–84. doi:10.1016/j.dsr2.2014.03.015

Palmer, M. A., Saenz, B. T., & Arrigo, K. R. (2014). Impacts of sea ice retreat, thinning, and melt-pond proliferation on the summer phytoplankton bloom in the Chukchi Sea, Arctic Ocean. *Deep Sea Research Part II: Topical Studies in Oceanography*, 105(C), 85–104. doi:10.1016/j.dsr2.2014.03.016

Pickart, R. S., Weingartner, T. J., Pratt, L. J., Zimmermann, S., & Torres, D. J. (2005). Flow of winter-transformed Pacific water into the Western Arctic. *Deep Sea Research Part II: Topical Studies in Oceanography*, 52(24-26), 3175–3198. http://doi.org/10.1016/j.dsr2.2005.10.009

Plourde, S., Campbell, R. G., Ashjian, C. J., & Stockwell, D. A. (2005). Seasonal and regional patterns in egg production of Calanus glacialis/marshallae in the Chukchi and Beaufort Seas during spring and summer, 2002. *Deep Sea Research Part II: Topical Studies in Oceanography*, 52(24-26), 3411–3426. doi:10.1016/j.dsr2.2005.10.013

Quakenbush, L. T., Citta, J. J., George, J. C., & Small, R. J. (2010). Fall and winter movements of bowhead whales (Balaena mysticetus) in the Chukchi Sea and within a potential petroleum development area. *Arctic*. http://doi.org/10.2307/20799597

Questel, J. M., Clarke, C., & Hopcroft, R. R. (2013). Continental Shelf Research. Continental Shelf Research, 67(C), 23–41. doi:10.1016/j.csr.2012.11.003

Railsback, S. F. & Grimm, V. (2011). *Agent-Based and Individual-Based Modeling: A Practical Introduction*. Princeton, NJ: Princeton University Press.

Rose, K. A., Roth, B. M., & Smith, E. P. (2009). Skill assessment of spatial maps for oceanographic modeling. *Journal of Marine Systems*, *76*(1-2), 34–48. http://doi.org/10.1016/j.jmarsys.2008.05.013

Sherr, E. B., Sherr, B. F., & Hartz, A. J. (2009). Microzooplankton grazing impact in the Western Arctic Ocean. *Deep Sea Research Part II: Topical Studies in Oceanography*, 56(17), 1264–1273. doi:10.1016/j.dsr2.2008.10.036

Sedláček, J., Knutti, R., Martius, O., & Beyerle, U. (2012). Impact of a Reduced Arctic Sea Ice Cover on Ocean and Atmospheric Properties. *Journal of Climate*, 25(1), 307–319. http://doi.org/10.1175/2011JCLI3904.1

Sherr, E. B., Sherr, B. F., & Hartz, A. J. (2009). Microzooplankton grazing impact in the Western Arctic Ocean. *Deep Sea Research Part II: Topical Studies in Oceanography*, 56(17), 1264–1273. http://doi.org/10.1016/j.dsr2.2008.10.036

Sherr, E. B., Sherr, B. F., & Ross, C. (2013). Microzooplankton grazing impact in the Bering Sea during spring sea ice conditions. *Deep Sea Research Part II: Topical Studies in Oceanography*, 94(C), 57–67. doi:10.1016/j.dsr2.2013.03.019

Smagorinsky, J. (1964). Some aspects of the general circulation. *Quarterly Journal Of The Royal Meteorological Society*, 90(383), 1. doi:10.1002/qj.49709038302

Spall, M. A. (2007). Circulation and water mass transformation in a model of the Chukchi Sea. *Journal of Geophysical Research*, 112(C5), C05025. doi:10.1029/2005JC003364

Spall, M. A., Pickart, R. S., Brugler, E. T., Moore, G. W. K., Thomas, L., & Arrigo, K. R. (2014). Role of shelfbreak upwelling in the formation of a massive under-ice bloom in the Chukchi Sea. *Deep Sea Research Part II: Topical Studies in Oceanography*, 105(C), 17–29. doi:10.1016/j.dsr2.2014.03.017

Søreide, J. E., Leu, E., Berge, J., Graeve, M., & Falk-Petersen, S. (2010). Timing of blooms, algal food quality and Calanus glacialis reproduction and growth in a changing Arctic. *Global Change Biology*, 16(11), no–no. http://doi.org/10.1111/j.1365-2486.2010.02175.x

Von Appen, W. J., & Pickart, R. S. (2012). Two Configurations of the Western Arctic Shelfbreak Current in Summer. *Journal of Physical Oceanography*, 42(3), 329–351. doi:10.1175/JPO-D-11-026.1

Walsh, J. J., Dieterle, D. A., Maslowski, W., Grebmeier, J. M., Whitledge, T. E., Flint, M., et al. (2005). A numerical model of seasonal primary production within the Chukchi/Beaufort Seas. *Deep Sea Research Part II: Topical Studies in Oceanography*, 52(24-26), 3541–3576. doi:10.1016/j.dsr2.2005.09.009

Wang, Jian, Cota, G. F., & Comiso, J. C. (2005). Phytoplankton in the Beaufort and Chukchi Seas: Distribution, dynamics, and environmental forcing. *Deep Sea Research Part II: Topical Studies in Oceanography*, 52(24-26), 3355–3368. doi:10.1016/j.dsr2.2005.10.014

Wang, Jia, Hu, H., Goes, J., Miksis-Olds, J., Mouw, C., D'Sa, E., et al. (2013). A modeling study of seasonal variations of sea ice and plankton in the Bering and Chukchi Seas during 2007-2008. *Journal of Geophysical Research: Oceans*, 118(3), 1520–1533. doi:10.1029/2012JC008322

Wassmann, P., & Reigstad, M. (2011). Future Arctic Ocean Seasonal Ice Zones and Implications for Pelagic-Benthic Coupling. *Oceanography*, (3), 220.

Wold, A. (2012). *Calanus glacialis – the role of lipids in the life cycle and for the Arctic pelagic food web*. (Unpublished doctoral dissertation). University of Tromsø, Tromsø, Norway.

Wold, A., Darnis, G., Søreide, J. E., Leu, E., Philippe, B., Fortier, L., et al. (2011). Life strategy and diet of Calanus glacialis during the winter–spring transition in Amundsen Gulf, southeastern Beaufort Sea. *Polar Biology*, 34(12), 1929–1946. http://doi.org/10.1007/s00300-011-1062-6

Woodgate, R. A., Aagaard, K., & Weingartner, T. J. (2005). A year in the physical oceanography of the Chukchi Sea: Moored measurements from autumn 1990–1991. *Deep Sea Research Part II: Topical Studies in Oceanography*, 52(24-26), 3116–3149. doi:10.1016/j.dsr2.2005.10.016

Weingartner, T., Dobbins, E., Danielson, S., Winsor, P., Potter, R., & Statscewich, H. (2013). Continental Shelf Research. *Continental Shelf Research*, 67(C), 5–22. doi:10.1016/j.csr.2013.03.012

Woodgate, R. A., Aagaard, K., & Weingartner, T. J. (2005). A year in the physical oceanography of the Chukchi Sea: Moored measurements from autumn 1990–1991. *Deep Sea Research Part II: Topical Studies in Oceanography*, 52(24-26), 3116–3149. http://doi.org/10.1016/j.dsr2.2005.10.016

Zhang, J., Spitz, Y. H., Steele, M., Ashjian, C., Campbell, R., Berline, L., & Matrai, P. (2010). Modeling the impact of declining sea ice on the Arctic marine planktonic ecosystem. *Journal of Geophysical Research*, 115(C10), C10015. doi:10.1029/2009JC005387